

$T\bar{T}$ deformations from AdS_2 to dS_2

Sergio E. Aguilar-Gutierrez,^{a,b} Andrew Svesko,^c and Manus R. Visser^d

^a*Okinawa Institute of Science and Technology Graduate University, Onna, Okinawa 904 0495, Japan*

^b*Institute for Theoretical Physics, KU Leuven, Celestijnenlaan 200D, B-3001 Leuven, Belgium*

^c*Department of Mathematics, King's College London, Strand, London WC2R 2LS, UK*

^d*Institute for Mathematics, Astrophysics and Particle Physics, and Radboud Center for Natural Philosophy, Radboud University, 6525 AJ Nijmegen, The Netherlands*

E-mail: sergio.ernesto.aguilar@gmail.com, andrew.svesko@kcl.ac.uk,
manus.visser@ru.nl

ABSTRACT: We revisit the formalism of $T\bar{T}$ deformations for quantum theories that are holographically dual to two-dimensional dilaton-gravity theories with Dirichlet boundary conditions. To better understand the microscopics of de Sitter space, we focus on deformations for which the dual bulk geometry flows from Anti-de Sitter to de Sitter space. We explore two distinct ways to achieve this: either through so-called centaur geometries that interpolate between AdS_2 and dS_2 , or by a spherical dimensional reduction of $T\bar{T} + \Lambda_2$ theories that were proposed to give a microscopic interpretation of three-dimensional de Sitter entropy. We derive the microscopic energy spectrum, heat capacities, and deformed Cardy expressions for the thermodynamic entropy in the canonical and microcanonical ensembles for these two setups. In both setups a signature of the change from AdS to dS is that the heat capacity at a fixed deformation parameter of the boundary system changes sign, indicating the existence of a thermodynamically unstable de Sitter patch. Our findings provide important consistency conditions for holographic models of the dS_2 static patch.

Contents

1	Introduction	1
2	Quasi-local thermodynamics in general dilaton-gravity	4
2.1	General 2D dilaton-gravity with Dirichlet walls	4
2.2	$T\bar{T}$ deformations and the microscopic energy spectrum	11
2.3	$T\bar{T}$ deformation for theories dual to general 2D dilaton theories	15
2.4	Cardy-like formulae for the thermal entropy of the dual deformed theory	17
3	Interpolating geometries via $T\bar{T}$ deformations	20
3.1	Centaur (A)dS ₂ geometries	20
3.2	Thermodynamics of the dual deformed theory	22
4	Dilaton gravity from $T\bar{T} + \Lambda_2$	25
4.1	Review of $T\bar{T} + \Lambda_2$ deformations and patchwise holography	26
4.2	Generalizing $T\bar{T} + \Lambda_2$ to arbitrary energies: from BTZ to conical dS ₃	28
4.3	Dimensional reduction of $T\bar{T} + \Lambda_2$	31
5	Discussion and Outlook	34
A	Flow equations dual to general 2D dilaton gravity	36

1 Introduction

Like black hole horizons, the cosmological horizon of de Sitter (dS) space obeys an entropy-area law [1, 2],

$$S_{\text{GH}} = \frac{A}{4G}. \tag{1.1}$$

Here S_{GH} denotes the thermal entropy associated to the dS static patch, where A is the cross-sectional area of the horizon. The thermodynamic description of dS, however, is far more subtle than its asymptotically flat or anti-de Sitter (AdS) black hole counterparts. Indeed, unlike black holes, adding positive energy to the dS static patch at fixed cosmological constant leads to an entropy reduction, as follows from an additional minus sign appearing in the first law of cosmological horizons [1]. Moreover, spatial sections of dS space are spheres, having no asymptotic boundary, such that the total gravitational energy (defined with respect to the time translation Killing vector of the static patch) vanishes. Additionally, the microscopic origin of Gibbons-Hawking entropy (1.1) is more mysterious than for black holes. Due to the

apparent lack of unbroken supersymmetry in empty dS [3–5], it seems unlikely the string-theoretic explanation for the entropy of specific black holes [6, 7] applies to dS horizons.

A promising way to address all of these puzzles is to introduce a finite timelike boundary satisfying Dirichlet boundary conditions inside the dS static patch, extending previous work by York and collaborators [8–13]. The Dirichlet wall delineates two distinct systems: the “horizon patch”, the region between the wall and the horizon, and the “pole patch”, the region between the wall and the pole. Thermal ensembles may then be consistently defined by fixing quasi-local thermodynamic data with respect to the Dirichlet wall [14] (see also [15–19]). The quasi-local set-up also reveals the origin of the minus sign in the first law of cosmological horizons is a consequence of misinterpreting matter Killing energy as the internal energy of the system [20].

Timelike Dirichlet walls, moreover, provide a natural home for holographic quantum theories dual to a finite region of bulk gravity. Indeed, this is one approach to provide a holographic description of the de Sitter static patch. Specifically, in [21, 22] it was proposed that the non-gravitating dual theory resides on a timelike boundary near the pole of de Sitter space, whereas in [23] the dual description lives on the (stretched) cosmological horizon. Our perspective is that a Dirichlet wall can interpolate between these two proposals since it can sit at any location in de Sitter static patch [17, 24]. Holography of timelike Dirichlet boundaries thus offers a way to explore the microscopic origins of de Sitter thermodynamics.

Indeed, Dirichlet walls play a critical role in providing a microstate accounting of the Gibbons-Hawking entropy, including its 1-loop logarithmic correction [25–28]. Broadly, the idea is to start with an AdS₃ black hole near the Hawking-Page (HP) transition and push its asymptotic timelike boundary inward until positioned just outside of the black hole horizon, where it becomes indistinguishable from the dS₃ cosmological horizon. The timelike boundary is then pushed outward in a specific way to recover the dS static patch geometry. This procedure, in three bulk spacetime dimensions, has a dual description in terms of solvable deformations of two-dimensional conformal field theories (CFT) living on the Dirichlet wall. Precisely, pushing the AdS₃ boundary inward corresponds to an irrelevant $T\bar{T}$ deformation of a holographic CFT₂ [29–34], while a $T\bar{T} + \Lambda_2$ deformation builds the dS₃ static patch [25–28, 35]. With this patch-wise prescription, “dressed” microstates of the AdS₃ black hole are identified with the microstates associated with the dS₃ static patch, such that the dS₃ entropy is exactly equal to the Cardy entropy of the dual CFT₂. Thence, analogous to AdS₃ black holes [36, 37],¹ the Gibbons-Hawking entropy of dS₃ follows from a counting of dual CFT microstates, consistent with a different approach using the long-string phenomenon [24].

In this article we develop a dual holographic description for the quasi-local thermodynamics of two-dimensional de Sitter space. We do so by adapting the $T\bar{T}$ formalism dual to bulk geometric flows from AdS₂ to dS₂. In particular, we study the properties of the microscopic theory dual to the “centaur” model [22], a specific two-dimensional model of dilaton gravity,

¹A similar conclusion is reached for Kerr-dS₃ [38], where, via dS₃/CFT₂ duality, the cosmological horizon entropy equals the Cardy entropy [39] of CFT₂ deformed by a marginal operator located at past infinity.

that describes an interpolation between AdS_2 and dS_2 . Further, we holographically characterize a similar type of geometric flow via a one-dimensional analog of $\text{T}\bar{\text{T}} + \Lambda_2$ -deformations.

More precisely, we first revisit a conjectured microscopic description of the quasi-local energy for a general class of two-dimensional dilaton theories of gravity [40]. The correspondence essentially follows from a dimensional reduction of $\text{T}\bar{\text{T}}$ -deformations to a two-dimensional holographic CFT. Within this framework, we provide the first dual holographic description of the quasi-local thermodynamics of Jackiw-Teitelboim (JT) gravity [41, 42] in de Sitter space [17], and the centaur model [19]. In particular, we find that the microcanonical entropy of the dual deformed theory of the dS_2 geometry has a Cardy-like form (cf. (2.58)),

$$S(\lambda, \mathcal{E}) = S_0 \pm 2\pi \sqrt{\frac{c}{6} \left(\mathcal{E}(\lambda\mathcal{E} - 2) + \frac{2}{\lambda} \right)} \iff S_{\text{BH}} = \frac{\Phi_0}{4G_2} + \frac{\Phi_h}{4G_2}, \quad (1.2)$$

where ‘+’ refers to states dual to the patch in dS_2 between the Dirichlet wall and the cosmological horizon, and ‘-’ to states dual to the patch between the Dirichlet boundary and the black hole horizon. Further, \mathcal{E} is a (dimensionless) microscopic energy, λ is a dimensionless parameter characterizing the $\text{T}\bar{\text{T}}$ -flow, and c is the one-dimensional analog of a central charge of the seed ($\lambda = 0$) conformal quantum theory. Note that the microcanonical entropy reduces to the Cardy formula for $\lambda = 1/\mathcal{E} = 1/(2\mathcal{E}_0)$, for energy \mathcal{E}_0 of the undeformed theory (where the Dirichlet wall is located at the horizon). Applying the appropriate holographic dictionary, we recover the classical gravitational entropy of dS_2 (2.13), where Φ_0 is proportional to S_0 and Φ_h is the value of the dilaton at either the black hole or cosmological horizon. Further, we compute the microscopic energy spectrum and heat capacity, finding that the boundary dual to the dS_2 cosmic patch is thermally unstable (see also [14, 17, 19]).

We further consider a spherical dimensional reduction of a generalized $\text{T}\bar{\text{T}} + \Lambda_2$ flow connecting a BTZ black hole of arbitrary mass to a locally conical dS_3 spacetime. This leads us to a new type of flow connecting AdS_2 and dS_2 along their respective horizons, in contrast with the centaur model. Moreover, the AdS_2 region in this case corresponds to an eternal AdS_2 black hole (i.e., Rindler- AdS_2), whereas the AdS_2 region in the centaur geometry corresponds to global AdS . Consequently, the thermal entropy of states dual to AdS_2 regions differ from those in the centaur model. The quasi-local heat capacities of the interpolating system are qualitatively the same as the centaur model, however. In particular, the boundary dual to the AdS_2 black hole that is smoothly connected to the seed theory is thermally stable, while the boundary dual to the cosmic patch dS_2 solution is unstable.

The remainder of this article is as follows. In Section 2 we study $\text{T}\bar{\text{T}}$ deformed theories dual to general dilaton-gravity models; reviewing the procedure developed in [40] and adapting it to (A)dS JT gravity. We derive the microscopic energy spectrum, thermodynamic entropy and heat capacity, finding precise agreement with the bulk quasi-local thermodynamics. We provide a dual holographic description of the centaur model in terms $\text{T}\bar{\text{T}}$ -flows in Section 3. In Section 4, we first generalize $\text{T}\bar{\text{T}} + \Lambda_2$ deformations connecting a BTZ black hole of arbitrary

mass to a locally conical dS_3 spacetime of the same mass.² We then dimensionally reduce this flow, leading to another type of geometric flow between (A)dS₂ patches, and analyze the quasi-local thermodynamics. We conclude in Section 5 with a summary and discussion of future work. Appendix A provides explicit details deriving the flow equation and microscopic energy spectrum for deformed theories dual to general 2D dilaton theories of gravity.

2 Quasi-local thermodynamics in general dilaton-gravity

In this section, we summarize essential elements of the thermodynamics of general 2D dilaton-gravity theories with Dirichlet walls and the one-dimensional analog of $T\bar{T}$ deformations. We follow the previous work [17, 19, 40, 43] in this section, highlighting aspects that have not been analyzed in the literature.

2.1 General 2D dilaton-gravity with Dirichlet walls

Pure general relativity in two dimensions is topological, having trivial dynamics. However, 2D dilaton-gravity theories have nontrivial dynamics and are characterized by actions of the type (in Euclidean signature)

$$I_E = I_{\text{top}} - \frac{1}{16\pi G_2} \int_{\mathcal{M}} d^2x \sqrt{g} (R\Phi + V(\Phi)) - \frac{1}{8\pi G_2} \int_{\partial\mathcal{M}} d\tau \sqrt{h} \Phi K + I_{\text{ct}} , \quad (2.1)$$

with the topological term

$$I_{\text{top}} = -\frac{\Phi_0}{16\pi G_2} \int_{\mathcal{M}} d^2x \sqrt{g} R - \frac{\Phi_0}{8\pi G_2} \int_{\partial\mathcal{M}} d\tau \sqrt{h} K = -\frac{2\pi}{8\pi G_2} \Phi_0 \chi , \quad (2.2)$$

and I_{ct} is a counterterm action. The theory consists of a contribution over bulk spacetime \mathcal{M} endowed with metric $g_{\mu\nu}$, and a (timelike) boundary $\partial\mathcal{M}$ term, with induced metric $h_{\mu\nu}$ and (trace of) extrinsic curvature K . In Euclidean signature, we take \mathcal{M} to have the topology of a disk, such that $\partial\mathcal{M} = S^1$. The dilaton Φ ,³ resides on all of \mathcal{M} including $\partial\mathcal{M}$, and has general potential $V(\Phi)$. The contribution (2.2), with positive, dimensionless constant $\Phi_0 \gg \Phi$ and Euler character χ of \mathcal{M} , describes a topological contribution, having no effect on the gravitational dynamics, though it will contribute to the thermodynamics. All interesting dynamics arise from the remaining terms in (2.1), with the third being the Gibbons-Hawking-York contribution, while the fourth I_{ct} is a local counterterm rendering the action finite. For our purposes, since we are interested in 2D geometries with an AdS₂ boundary, the counterterm is

$$I_{\text{ct}}^{\text{JT}} = \frac{1}{8\pi G_2} \int_{\partial\mathcal{M}} d\tau \sqrt{h} \frac{\Phi}{\ell} . \quad (2.3)$$

²A version of this more general flow was considered in [26]. Specifically, flows dual to gluing the BTZ geometry to dS_3 with a conical *excess*.

³Newton's constant G_2 is dimensionless in two spacetime dimensions, but we keep it for bookkeeping purposes. In fact, the prefactor $(\Phi_0 + \Phi)$ plays the natural role of a gravitational constant, where a diverging dilaton indicates regions of weak gravity.

with ℓ being a bulk curvature scale (determined by the dilaton potential $V(\Phi)$, as in (2.5)).

Models of the type (2.1) have a higher-dimensional pedigree for specific dilaton potentials and asymptotic structure. In particular, when $V(\Phi) = +2\Phi/\ell^2$, the action is that of AdS₂ Jackiw-Teitelboim (JT) gravity [41, 42], which follows from a spherical-dimensional reduction of black hole spacetimes whose extremal limit takes the form AdS₂ \times X for compact space X . In this context, the dilaton Φ controls the size of X , and thus represents (small) deviations away from extremality. The resulting 2D geometry describes an AdS₂ black hole, with horizon entropy $S_{\text{BH}} = (\Phi_0 + \Phi_h)/4G_2$, where Φ_0 corresponds to the extremal entropy of the higher-dimensional black hole, and Φ_h is the value of the dilaton evaluated at the AdS₂ black hole horizon. Analogously, the potential $V(\Phi) = -2\Phi/\ell^2$ yields dS₂ JT gravity, which follows from a spherical reduction of higher-dimensional de Sitter black holes in their near-horizon, near-Nariai limit, which has the product structure dS₂ \times X , and Φ represents deviations from the Nariai limit, where the cosmological and black hole horizons coincide [17, 44]. The 2D spacetime can be interpreted as a dS₂ black hole, where Φ_0 is proportional to the entropy of the higher-dimensional Nariai black hole. We will be interested in 2D spacetimes which interpolate between AdS₂ and dS₂, corresponding to an interpolation between the dilaton potentials characterizing (A)dS₂ JT gravity [19, 22].

The gravitational and dilaton equations of motion of (2.1) are, respectively,

$$\nabla_\mu \nabla_\nu \Phi - g_{\mu\nu} \nabla^2 \Phi + \frac{1}{2} g_{\mu\nu} V(\Phi) = 0, \quad (2.4)$$

$$R = -\partial_\Phi V(\Phi). \quad (2.5)$$

Clearly, the gravity equation of motion governs the dynamics of the dilaton, while the dilaton equation of motion fixes the background metric. A general solution to the equations of motion can be written in the form (cf. [45])

$$ds^2 = N(r) d\tau^2 + \frac{dr^2}{N(r)}, \quad \Phi = \Phi_r \frac{r}{\ell}, \quad (2.6)$$

for positive, dimensionless constant Φ_r . We further impose $\Phi_0 \gg \Phi_r$; for theories that arise from a dimensional reduction, this condition is a direct consequence of the parent geometry being a nearly-extremal black hole. The Ricci scalar of the metric is $R = -\partial_r^2 N(r)$ such that

$$N(r, r_h) = \frac{\ell}{\Phi_r} \int_{r_h}^r dr' V(r'). \quad (2.7)$$

These types of solutions describe a 2D Euclidean geometry with r_h as the location of its horizon, where $N(r_h, r_h) = 0$ and $N(r, r_h) > 0$ for all $r \neq r_h$ such that the geometry is Euclidean. Additionally, the period of Euclidean time τ is $\tau \sim \tau + \beta_{\text{H}}$, where

$$\beta_{\text{H}} = \frac{4\pi\Phi_r}{\ell|V(r_h)|} \quad (2.8)$$

upon expanding (2.6) near r_h and removing the conical singularity at r_h .⁴

⁴The period β_{H} coincides with the inverse of the Hawking temperature, $\beta_{\text{H}} = 2\pi/\kappa = 4\pi/|N'(r_h)|$, for surface gravity κ , defined by $\xi^\mu \nabla_\mu \xi^\nu = \kappa \xi^\nu$ on the horizon with respect to the Killing field $\xi = \partial_\tau$.

Some additional care is needed depending on whether we are describing a geometry with a black hole or cosmological horizon (both feature in de Sitter JT gravity). In either case, being a Euclidean section requires $N(r, r_h) > 0$ for all $r \neq r_h$. As written, (2.7) is non-negative for $r \geq r_h$, with r_h denoting the black hole horizon. Alternatively, for systems with a cosmological horizon $r_c \geq r$, one instead has $N(r, r_c) \propto \int_r^{r_c} dr' V(r') < 0$ [19].

Adding a Dirichlet wall and quasi-local thermodynamics

Now we impose Dirichlet boundary conditions at the boundary $\partial\mathcal{M}$ that fix the proper length β_T of \mathcal{M} , and the value of the dilaton at the boundary, $\Phi = \Phi_B$ [17, 19, 46, 47]. On-shell, the value of the dilaton is proportional to the coordinate radius, $\Phi_B \propto r_B$. Hence, on-shell, fixing Φ_B amounts to fixing r_B . While the former boundary data properly defines the ensemble and is covariant, we often express thermodynamic quantities also in terms of r_B for convenience when we relate the quasi-local thermodynamics to $\overline{\text{T}\overline{\text{T}}}$ deformations. As pointed out above, the addition of a Dirichlet wall allows for a proper definition of thermal ensembles when the spacetime has a cosmological horizon. Indeed, Euclidean de Sitter space is a sphere, having no boundary, such that there is no location to fix thermodynamic data defining a thermal ensemble, as occurs in, for example, asymptotically AdS or flat black hole backgrounds. The Dirichlet wall thus provides a location to fix the data defining a thermal ensemble.

In 2D dilaton gravity, the solutions for the metric and dilaton with these boundary conditions are given by (2.6). The periodicity of the Euclidean time is β_H , but the proper length of the time circle at $\partial\mathcal{M}$, which is fixed to be β_T , is equal on-shell to the inverse of the Tolman temperature $T = \beta_T^{-1}$,

$$\beta_T(r_B) = \int_0^{\beta_H} d\tau \sqrt{N(r_B, r_h)} = \beta_H \sqrt{N(r_B, r_h)}. \quad (2.9)$$

Clearly, T is the redshifted temperature locally measured at $\partial\mathcal{M}$.

Following the standard Gibbons-Hawking analysis [2], the canonical partition function $Z(\beta_T)$ is represented as a Euclidean gravitational path integral, with integration measure over all the dynamical fields ($g_{\mu\nu}$ and Φ) with the same Dirichlet boundary conditions defining the ensemble. In a semi-classical saddle-point approximation, the partition function is given by $Z(\beta_T) \approx e^{-I_E}$, for on-shell action I_E . Specifically, for a system with a single black hole horizon (we describe the case with a cosmological horizon momentarily), the Euclidean action (2.1) on-shell is [17, 19]

$$I_E = \frac{\beta_H \Phi_0}{16\pi G_2} \left(\int_{r_h}^{r_B} dr N''(r) - N'(r_B) \right) - \frac{\beta_H \Phi_r}{16\pi G_2 \ell} \int_{r_h}^{r_B} dr [-r N''(r) + N'(r)] - \frac{\beta_H \Phi_B}{16\pi G_2} N'(r_B) + I_{\text{ct}}, \quad (2.10)$$

where we used $K = N'/2\sqrt{N}$, the trace of the extrinsic curvature of the boundary $\partial\mathcal{M}$, and the prime denotes the derivative with respect to r . Evaluating and using integration by parts

in the second term yields

$$I_E = -\frac{1}{4G_2}(\Phi_0 + \Phi_h) - \beta_T \frac{\Phi_r \sqrt{N(r_B)}}{8\pi G_2 \ell} + \beta_T \frac{\Phi_B}{8\pi G_2 \ell}, \quad (2.11)$$

with $\Phi_h = \Phi(r_h)$ being the value of the dilaton at the black hole horizon. The third contribution is the counterterm action evaluated on shell. Using the identification $\log Z(\beta_T) = -I_E$ in the saddle point approximation, the energy and entropy can be computed from the Euclidean on-shell action as follows

$$E_{\text{BY}} = \left(\frac{\partial I_E}{\partial \beta_T} \right)_{\Phi_B} = \frac{\Phi_r}{8\pi G_2 \ell} \left(r_B/\ell - \sqrt{N(r_B)} \right), \quad (2.12)$$

$$S_{\text{BH}} = \beta_T \left(\frac{\partial I_E}{\partial \beta_T} \right)_{\Phi_B} - I_E = \frac{\Phi_0 + \Phi_h}{4G_2}, \quad (2.13)$$

where we used $\partial_{r_h} N(r_B, r_h) = -\ell V(r_h)/\Phi_r$ together with the chain rule $\partial_{\beta_T} = (\partial \beta_T / \partial r_h)^{-1} \partial_{r_h}$.⁵ Here, E_{BY} is the quasi-local thermodynamic energy, which can also be computed using the Brown-York stress-energy tensor [11], see, e.g., equation (3.4) in [17]. The on-shell Euclidean action (2.11) is thus proportional to the free energy

$$I_E = \beta_T F = \beta_T E_{\text{BY}} - S_{\text{BH}}. \quad (2.14)$$

Further, the heat capacity at fixed Φ_B is

$$C_{\Phi_B} \equiv -\beta_T^2 \left(\frac{\partial E_{\text{BY}}}{\partial \beta_T} \right)_{\Phi_B} = \frac{\beta_T \Phi_r}{8\pi G_2 \ell} \frac{\sqrt{N(r_B)} V(r_h)^2}{(V(r_h)^2 + 2N(r_B)V'(r_h)\Phi_r/\ell)}, \quad (2.15)$$

matching [19, 48]. We also define a ‘‘surface pressure’’ σ

$$\sigma \equiv - \left(\frac{\partial E_{\text{BY}}}{\partial \Phi_B} \right)_{S_{\text{BH}}} = \frac{1}{8\pi G_2} \left(\frac{1}{\ell} - \frac{N'(r_B)}{2\sqrt{N(r_B)}} \right), \quad (2.16)$$

with fixed entropy S_{BH} (equivalently, fixed r_h). The quasi-local energy, gravitational entropy, and surface pressure together obey the quasi-local first law for 2D dilaton-gravity [17]

$$dE_{\text{BY}} = T dS_{\text{BH}} - \sigma d\Phi_B. \quad (2.17)$$

(A)dS₂ JT gravity

For concreteness, let us apply the above formalism to two specific theories.

AdS₂: First consider the case of AdS₂ JT gravity, characterized by Euclidean action (2.1), with potential $V(\Phi) = 2\Phi/\ell^2$. The blackening factor is

$$N(r, r_h) = (r^2 - r_h^2)/\ell^2, \quad (2.18)$$

⁵It is useful to know

$$\left(\frac{\partial \beta_T}{\partial r_h} \right) = -\frac{\beta_T}{N(r_B)} \frac{[\ell V(r_h)^2 + 2\Phi_r V'(r_h)N(r_B)]}{2\Phi_r V(r_h)}.$$

and the Ricci scalar is $R = -2/\ell^2$, such that the background is an eternal AdS₂ black hole. The (inverse) Tolman temperature is $\beta_T = \frac{\beta_H}{\ell} \sqrt{r_B^2 - r_h^2}$, with $\beta_H = 2\pi\ell^2/r_h$. Further, the quasi-local energy (2.12) takes the form

$$E_{\text{BY}} = \frac{\Phi_B}{8\pi G_2 \ell} \left(1 - \frac{\beta_T}{\sqrt{4\pi^2 \ell^2 + \beta_T^2}} \right) = \frac{\Phi_r}{8\pi G_2 \ell^2} \left(r_B - \sqrt{r_B^2 - r_h^2} \right). \quad (2.19)$$

The energy is non-negative for all temperatures $\beta_T \in [0, \infty)$ (or for $r_B \geq r_h$). Notice the quasi-local energy multiplied by the lapse $\sqrt{N(r_B)}$ and taking the $r_B \rightarrow \infty$ limit yields the black hole ADM mass [49, 50],

$$M_{\text{ADM}} = \frac{\Phi_r r_h^2}{16\pi G_2 \ell^3}. \quad (2.20)$$

Notice also that, without multiplying by the lapse, for large r_B the quasi-local energy takes the form $M_{\text{ADM}}\ell/r_B$, which is according to the holographic dictionary [51–53] the dimensionful energy in the dual boundary theory.

Meanwhile, the heat capacity (2.15),

$$C_{\Phi_B} = \frac{4\pi^2 \ell \Phi_B}{8\pi G_2} \frac{\beta_T^2}{(4\pi^2 \ell^2 + \beta_T^2)^{3/2}}, \quad (2.21)$$

is positive everywhere for $\beta_T > 0$, except at $\beta_T = 0$ where it vanishes. Hence, the AdS₂ black hole system with a Dirichlet boundary is thermodynamically stable.

dS₂: Now consider the case of dS₂ JT gravity. The JT action (2.1), with potential $V(\Phi) = -2\Phi/\ell^2$, follows from a spherical dimensional reduction of four or higher-dimensional de Sitter-Schwarzschild black hole in its near-horizon, near-Nariai limit (see, e.g., [17, 44, 54, 55]). The solution to the equations of motion has Ricci scalar $R = +2/\ell^2$, such that the geometry is dS₂, namely, metric (2.6) with blackening factor

$$N(r_H, r) = (r_H^2 - r^2)/\ell^2, \quad \text{with} \quad -r_H \leq r \leq r_H \quad \text{for} \quad r_H > 0. \quad (2.22)$$

The essential new feature with this set-up is that dS₂ has two horizons: a black hole horizon $r_h = -r_H$ and a cosmological horizon $r_c = r_H$ with $r_H > 0$,⁶ a herald of the higher-dimensional origin. A Penrose diagram for this geometry is shown in Figure 1.

Now introduce a timelike Dirichlet wall inside the static patch in between the two horizons, i.e., $r_B \in [r_h, r_c]$. The quasi-local thermodynamics of this model was studied previously in [17, 19]. The wall divides the static patch into two systems: the black hole system, $r \in [r_h, r_B]$, and the cosmological system $r \in [r_B, r_c]$. Treating each system separately gives⁷

$$\log Z_{c,h}(\beta_T) = -\beta_T E_{\text{BY}}^{c,h} + S_{c,h}, \quad (2.23)$$

⁶In [17] $r_H = \ell$. Here we leave r_H as an independent parameter.

⁷For the black hole system, the on-shell action is as in (2.11). Alternatively, to evaluate the on-shell action of the cosmological system, first note that the Gibbons-Hawking boundary term comes with a sign change since the outward pointing normal vector of the cosmological horizon has an opposite orientation to that of the black hole horizon. Additionally, the r -integration range is $r \in [r_B, r_c]$.

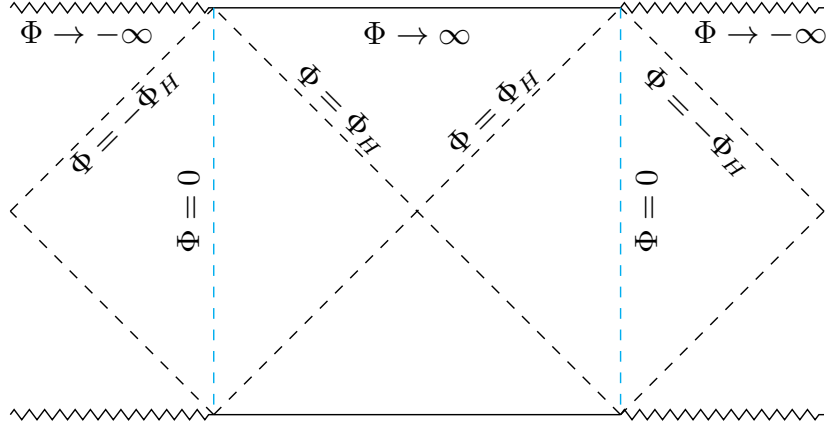


Figure 1: Full reduction model in dS_2 JT gravity. The black hole and cosmological horizons (black dashed lines) are located where $\Phi \rightarrow -\Phi_H$ and $\Phi \rightarrow +\Phi_H$. We have chosen the center of the static patches (cyan dashed lines) where $\Phi \rightarrow 0$.

where the inverse Tolman temperature, horizon entropy and quasi-local energies are, respectively, given on-shell by⁸

$$\beta_T = \frac{\beta_H}{\ell} \sqrt{r_H^2 - r_B^2} \quad (2.24)$$

$$S_{c,h} = \frac{1}{4G_2} (\Phi_0 \pm \Phi_H) \quad (2.25)$$

$$E_{\text{BY}}^{c,h} = \frac{1}{8\pi G_2 \ell} \left(\Phi_B \pm \frac{|\Phi_B| \beta_T}{\sqrt{4\pi^2 \ell^2 - \beta_T^2}} \right) = \frac{\Phi_r}{8\pi G_2 \ell^2} \left(r_B \pm \sqrt{r_H^2 - r_B^2} \right), \quad (2.26)$$

where $\beta_H = 2\pi\ell^2/r_H$ and $\Phi_H = r_H\Phi_r/\ell$. In both entropy and energy, the ‘+’ sign refers to the cosmological system while the ‘-’ sign corresponds to the black hole system. Geometrically, the ‘±’ sign reflects the sign change of the outward pointing normal vector n^α to $\partial\mathcal{M}$, since the quasi-local energy (without counterterm) is defined in JT gravity as $E_{\text{BY}} = -\frac{1}{8\pi G_2} n^\alpha \partial_\alpha \Phi$ [17]. Further, our expression for the quasi-local energy (2.26) differs from [17, 19] as here we have included a local counterterm, since later we will embed dS_2 inside an asymptotically AdS_2 background.⁹ The quasi-local energy of the cosmological system is real and non-negative when $\beta_T \in [0, 2\pi\ell]$. Similarly, for the black hole system the quasi-local energy is non-negative when $\beta_T \in [0, \sqrt{2}\pi\ell]$ and negative for $\beta_T > \sqrt{2}\pi\ell$. For $\beta_T > 2\pi\ell$, or equivalently for $r_B < -r_H$ and $r_B > r_H$, the energy of both systems becomes complex, i.e., when the Dirichlet wall is placed in the black hole interior or inflating patch, respectively. Further, multiplying the energy by the lapse and taking the limit as the wall approaches either horizon yields

⁸To arrive at the second equality in (2.26) we used $r_H = 2\pi\ell|r_B|/\sqrt{4\pi^2\ell^2 - \beta_T^2}$, which follows from inverting β_T for r_H .

⁹Without the counterterm, the quasi-local energy of the cosmological system is always non-negative, while it is always non-positive for the black hole system.

$\lim_{r_B \rightarrow r_{c,h}} \sqrt{N(r_B)} E_{\text{BY}}^{c,h} = 0$. This is in accordance with the standard Gibbons-Hawking result of vanishing energy in the dS static patch.

The heat capacity, meanwhile, is

$$C_{\Phi_B}^{c,h} = \mp \frac{4\pi^2 \ell |\Phi_B|}{8\pi G_2} \frac{\beta_{\text{T}}^2}{(4\pi^2 \ell^2 - \beta_{\text{T}}^2)^{3/2}}, \quad (2.27)$$

where the minus sign refers to the cosmological system and plus sign to the black hole system. Thus, while the heat capacity of the black hole system is *non-negative* everywhere in the range $\beta_{\text{T}} \in [0, 2\pi\ell]$ (or $r_B \in [-r_H, r_H]$), and hence thermally stable (at least locally), the heat capacity for the cosmological system is everywhere *non-positive* in the same range, indicating it is unstable against thermal fluctuations. Further, the black hole and cosmological systems represent two saddles to the Euclidean path integral, with the dominant one being the cosmological system as it has lower free energy, $F_h \geq F_c$, where $F_{c,h} = E_{\text{BY}}^{c,h} - T_{\text{T}} S_{c,h}$.

Note that dS₂ JT gravity also arises from a circular reduction of empty dS₃, leading to the so-called ‘‘half-reduction’’ model (opposed to the ‘‘full-reduction’’ model from near-Nariai de Sitter black holes considered here) [56, 57]. The essential geometric difference is that now the dS₂ geometry has no black hole horizon, whereas the static patch radial coordinate has the range $r \in [0, \ell]$. Moreover, $\Phi_0 = 0$, as there is no Nariai black hole from whence the 2D geometry came. Consequently, the Dirichlet wall divides the static patch into a ‘‘pole patch’’ (the region between the boundary and the pole $r = 0$) and ‘‘cosmic horizon patch’’ (the region between the cosmic horizon and the wall). The quasi-local thermodynamics of the cosmic horizon patch is identical to the cosmological system above, for the restricted range $r_B \in [0, r_H]$ [17]. In this article, however, we focus on the full-reduction model.

For AdS₂-JT gravity, the black hole horizon r_h is related to the ADM mass (2.20). Analogously, the dS₂ horizon radius r_H can be related to an ADM-like conserved charge as defined in [58]. This definition of mass for asymptotically dS _{$d+1$} spacetimes directly follows from constructing a quasi-local Brown-York stress tensor at early and late temporal infinity \mathcal{I}^\pm , i.e., outside the purview of a static patch observer. For example, consider the Schwarzschild-dS₃ conical defect

$$ds^2 = -N(r)d\tau^2 + \frac{dr^2}{N(r)} + r^2 d\phi^2, \quad (2.28)$$

with $N(r) = (8G_3 M - r^2/\ell^2)$, and cosmological horizon at $r_c = \ell\sqrt{8G_3 M}$. The parameter M is found to equal the ADM ‘mass’, computed from the quasi-local stress tensor outside the cosmological horizon ($r > \ell\sqrt{8GM}$) near \mathcal{I}^\pm .

Motivated by [58], which only considered pure Einstein-dS _{$d+1$} gravity for $d \geq 2$, we can extend their proposal to dS-JT gravity and define an ADM-like mass for asymptotically dS₂ geometries. To wit, Lorentzian dS₂ has line element

$$ds^2 = -N(r)dt^2 + N^{-1}(r)dr^2 \quad \text{with} \quad N(r) = (r_H^2 - r^2)/\ell^2. \quad (2.29)$$

Outside of the region accessible to a static patch observer, $r > r_c$, the coordinate r becomes timelike while t becomes a spatial coordinate, and \mathcal{I}^\pm are surfaces of large r . Using the

definition of the quasi-local Brown-York stress-tensor at a constant $r = r_B > r_c$ slice, the quasi-local energy takes the same form as for AdS₂ (2.19), with ADM mass (2.20), where r_h has been replaced by r_H .

2.2 $T\bar{T}$ deformations and the microscopic energy spectrum

3D/2D correspondence. Historically, $T\bar{T}$ deformations refer to the simplest example of solvable irrelevant deformations of a 2D CFT [30, 32]. This amounts to turning on a coupling μ resulting in a one-parameter family of local quantum field theories with Euclidean action

$$I_{\text{QFT}} = I_{\text{CFT}} + \mu \int d^2x \sqrt{\gamma} T\bar{T}(x), \quad (2.30)$$

where I_{CFT} is referred to as the ‘seed’ CFT, and $T\bar{T}(x)$ is a specific irrelevant, local, composite operator, given in terms of the quadratic product of the components of the deformed field theory stress-energy tensor T_{ij} :¹⁰

$$T\bar{T}(x) \equiv \frac{1}{8} [T^{ij}(x)T_{ij}(x) - (T_i^i(x))^2]. \quad (2.31)$$

Moreover, from $T_{ij} \equiv \frac{2}{\sqrt{\gamma}} \frac{\delta}{\delta \gamma^{ij}} I_{\text{QFT}}$, the deformed stress-tensor obeys $\gamma^{ij} T_{ij} = -2\mu T\bar{T}$. Incidentally, the deformation (2.31) preserves Lorentz invariance. The QFT generating function Z_{QFT} obeys

$$\partial_\mu \log Z_{\text{QFT}}(\mu) = - \int d^2x \sqrt{\gamma} \langle T\bar{T} \rangle, \quad (2.32)$$

where the initial condition of the flow is $Z_{\text{QFT}}(0) = Z_{\text{CFT}}$.

A key simplifying feature of $T\bar{T}$ deformations is that, for a finite μ , the expectation value of the composite operator in any translation invariant, stationary state factorizes as [29]

$$\langle T\bar{T} \rangle = \langle T \rangle \langle \bar{T} \rangle - \langle \Theta \rangle^2, \quad (2.33)$$

for $\Theta \equiv \frac{1}{4} T_i^i$. This factorization can be used to derive an exact renormalization group (RG) equation for the deformed theory, which coincides with a Hamilton-Jacobi equation whose classical limit corresponds to the Wheeler-DeWitt constraint characterizing the radial evolution of the three-dimensional gravity wavefunction [33]. Moreover, with respect to energy-momentum eigenstates $|n\rangle$ of the deformed Hamiltonian, the factorization (2.33) allows for an exact computation of the deformed energy spectrum. Specifically, in complex Cartesian coordinates $z = x + i\tau$ with Euclidean time τ ,

$$\langle n | T\bar{T} | n \rangle = -\frac{1}{4} [\langle n | T_{xx} | n \rangle \langle n | T_{\tau\tau} | n \rangle - \langle n | T_{x\tau} | n \rangle^2]. \quad (2.34)$$

¹⁰Technically $T\bar{T}$ is bilocal, $8T\bar{T}(x, y) = T^{ij}(x)T_{ij}(y) - T_i^i(x)T_j^j(y)$. Due to its OPE structure as $x \rightarrow y$, however, one typically works with the local operator $T\bar{T}(x)$ [29]. Further, in complex Cartesian coordinates $z = x + i\tau$, $8T\bar{T} = T_{zz}T_{\bar{z}\bar{z}} - (T_{z\bar{z}})^2 = \det(T_{ij})$, with trace $T_i^i = 4T_{z\bar{z}}$. Often one writes $T \equiv T_{zz}$, $\bar{T} \equiv T_{\bar{z}\bar{z}}$, and $T_{z\bar{z}} \equiv \Theta$, such that $8T\bar{T} = T\bar{T} - \Theta^2$. When the deformed CFT is another CFT, $T_i^i = 0$.

When the deformed CFT is on a cylinder with circumference L , one has a quantized energy $E_n \equiv L\langle n|T_{\tau\tau}|n\rangle$, pressure $\partial_L E_n \equiv \langle n|T_{xx}|n\rangle$, and momentum $iP_n = L\langle n|T_{\tau x}|n\rangle$, where the factor of i appears since $T_{zz} - T_{\bar{z}\bar{z}} = -iT_{x\tau}$. Moreover, from the (Euclidean) interaction Hamiltonian, one finds $\partial_\mu\langle H\rangle = L\langle T\bar{T}\rangle$, while $\partial_\mu P_n = 0$, since the momentum is quantized in units of $2\pi/L$.

Altogether, one finds the factorization (2.33) becomes the (forced inviscid) Burgers equation describing turbulent fluids,

$$4\partial_\mu E_n + E_n\partial_L E_n + \frac{P_n^2}{L} = 0. \quad (2.35)$$

Introducing the dimensionless parameter

$$\lambda \equiv \pi\mu/L^2, \quad (2.36)$$

the Burgers equation becomes

$$4\pi\partial_\lambda \mathcal{E}_n - 2\lambda\mathcal{E}_n\partial_\lambda \mathcal{E}_n - \mathcal{E}_n^2 + P_n^2 L^2 = 0, \quad (2.37)$$

with $\mathcal{E}_n = E_n L$. The solution is found to be [30, 32] (see also [29])

$$E_n(\lambda) = \frac{2\pi}{\lambda L} \left(1 - \sqrt{1 - 2\lambda M_n + \lambda^2 J_n^2} \right), \quad (2.38)$$

where the seed CFT gives the $\lambda = 0$ initial conditions, i.e., $E_n(\lambda = 0, L) = 2\pi M_n/L$ and $P_n = 2\pi J_n/L$. Using $M_n = \Delta_n + \bar{\Delta}_n - \frac{c}{12}$ and $J_n = \Delta_n - \bar{\Delta}_n$ for the undeformed CFT (where $(\Delta_n, \bar{\Delta}_n)$ are left and right scaling dimensions) the Casimir energy E_0 is

$$E_0(\lambda) = \frac{2\pi}{\lambda L} \left(1 - \sqrt{1 + \lambda \frac{c}{6}} \right), \quad (2.39)$$

where $\Delta_0 = \bar{\Delta}_0 = 0$, and c is the central charge of the seed CFT.

Since the deformed energy is monotonic in $(\Delta_n, \bar{\Delta}_n)$, the E_n levels do not intersect as μ or L are changed. This implies the thermal entropy of the deformed theory is independent of μ and, at high energies, given by the Cardy entropy of the undeformed CFT₂, i.e., $S_{\text{CFT}} = 2\pi\sqrt{\frac{c}{6}(\Delta_n - \frac{c}{24})} + 2\pi\sqrt{\frac{c}{6}(\bar{\Delta}_n - \frac{c}{24})}$.

Due to the square-root ‘shockwave singularity’ [30] that occurs for particular finite values of λ (where the square-root vanishes), the energy spectrum of the deformed QFT truncates above some critical value of the scaling dimension Δ_n , and places an upper bound on the energy and entropy. Thus, the deformed QFT on the cylinder has a finite number of quantum states [33], bounding the energy and entropy. Lastly, observe, outside of the square-root singularity, the deformed energy spectrum (2.38) takes complex values when $1 + \lambda^2 J_n^2 < 2\lambda M_n$.

When the deformed theory is taken to have a holographic dual,¹¹ it has been proposed the deformation represents a geometric cutoff in a three-dimensional asymptotically AdS space-time, where the QFT ends up residing on a Dirichlet wall at a fixed radial position r_B , such

¹¹The base assumption is to start with a holographic seed CFT₂ in a large- c and large ‘t Hooft coupling limit, where one is able to restrict to the universal sector captured by three-dimensional Einstein gravity.

that tuning the parameter μ amounts to tuning the position of the wall [33]. This proposal is based on a number of observations. Specifically, directly compare the deformed spectrum (2.38) to the Brown-York quasi-local energy of the Bañados-Teitelboim-Zanelli (BTZ) black hole [59, 60] of mass M_{ADM} , spin J and AdS₃ length scale ℓ_3 (cf. [13])

$$E_{\text{BY}}^{\text{BTZ}} = \frac{r_B}{4G_3\ell_3} \left(1 - \sqrt{1 - \frac{8G_3M_{\text{ADM}}\ell_3^2}{r_B^2} + \frac{16G_3^2\ell_3^2J^2}{r_B^4}} \right). \quad (2.40)$$

One finds precise agreement with the spectrum (2.38) upon invoking the standard AdS₃/CFT₂ dictionary to match the BTZ mass and angular momentum to the seed initial conditions, $\ell_3M_{\text{ADM}} = M_n$ and $J = J_n$, in addition to setting $L = 2\pi r_B$ and identifying $\lambda \equiv \frac{4G_3\ell_3}{r_B^2}$. At $\lambda = 0$ the BY energy reduces to $E_{\text{BY}}^{\text{BTZ}}(r_B \rightarrow \infty) = M_{\text{ADM}}\ell_3/r_B$, which is dual according to the holographic dictionary [51–53] to the (dimensionful) CFT₂ energy $2\pi M_n/L$. Thus, a $\text{T}\bar{\text{T}}$ flow starting at $\lambda = 0$ and increasing toward some fixed $\lambda > 0$ has a dual description as moving the AdS₃ conformal boundary inward from infinity to $r = r_B$.

Further, as demonstrated in the two-dimensional context, including a Dirichlet boundary does not alter the form of the horizon entropy: the thermal entropy of the black hole continues to follow the Bekenstein-Hawking area law, i.e., $S_{\text{BH}} = \frac{2\pi r_h}{4G_3}$ where r_h is the black hole horizon radius. This is consistent with the dual picture, where the entropy of the deformed field theory is still given by the Cardy entropy. Moreover, gravitationally speaking, the square root singularity in the deformed energy spectrum occurs when the Dirichlet wall approaches the location of the BTZ event horizon, $r_B \rightarrow r_h$, where the upper bound on energy and entropy coincide with a BTZ black hole which entirely fills the AdS₃ region cutoff at the wall.

Aside from matching the deformed energy spectrum to the quasi-local energy, additional non-trivial observations have been made relating bulk and boundary sides of the correspondence. These include computing propagation speeds of small perturbations about thermal states [33], and the computation of stress-tensor correlation functions [34].

Dimensional reduction to 2D/1D system. The goal now is to perform a similar analysis in one fewer dimension to provide a microscopic interpretation of the aforementioned quasi-local thermodynamics in AdS₂. This was accomplished by a dimensional reduction of $\text{T}\bar{\text{T}}$ deformations of two-dimensional CFTs [40, 43].¹² To this end, it proves useful to first rewrite the composite operator $\text{T}\bar{\text{T}}$ in the following way. Introduce angular coordinate θ such that the QFT metric is diagonal. Using $T_i^i = -2\mu\text{T}\bar{\text{T}}$ to solve for T_θ^θ , the flow equation for the deformed QFT action (2.30) becomes

$$\partial_\mu I_{\text{QFT}} = \int d^2x \sqrt{\gamma} \left(\frac{(T_\tau^\tau)^2 + T_{\tau\theta}T^{\tau\theta}}{4 - 2\mu T_\tau^\tau} \right). \quad (2.41)$$

A pole appears when $T_\tau^\tau = 2/\mu$; with $E = \int d\theta T_\tau^\tau = LT_\tau^\tau$, this pole coincides with the square-root singularity of the deformed spectrum (2.38). Moreover, with $iP_n = T_{\tau\theta}$, one recovers

¹²See also the dimensional reduction of massive gravity generalizations of stress-tensor deformations [61].

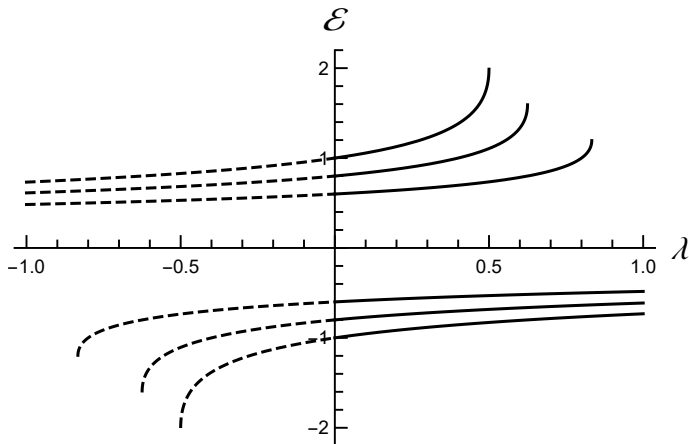


Figure 2: Energy levels \mathcal{E} of the dual theory to AdS_2 JT gravity with a finite cutoff at fixed \mathcal{E}_0 (2.44) (from top to bottom: $\mathcal{E}_0 = 1, .8, .6, -.6, -.8, -1$). Solid lines indicate $\lambda > 0$, while dashed lines correspond to $\lambda < 0$. This plot is qualitatively identical to energy levels of the 2D effective theory dual to AdS_3 gravity with a finite cutoff [33].

the flow equation (2.35). The advantage of recasting the deformations in this way is one may now perform a simple dimensional reduction of the two-dimensional equation (2.41) [40]. This amounts to setting $T_{r\theta} = 0$, or, equivalently, $P_n = J_n = 0$ in the deformed energy spectrum (2.38), yielding

$$\partial_\mu(E/L) = \frac{(E/L)^2}{4 - 2\mu E/L} \implies E(\lambda) = \frac{2\pi}{\lambda L} \left(1 - \sqrt{1 - 2\lambda\mathcal{E}_0}\right), \quad (2.42)$$

where the undeformed CFT energy M_n has been replaced by the $E(\lambda = 0) \equiv 2\pi\mathcal{E}_0/L$ energy of the one-dimensional seed quantum mechanical theory, whatever it may be (more on this later). The square-root singularity appears when $1 = 2\lambda\mathcal{E}_0$, while the spectrum goes complex if $2\lambda\mathcal{E}_0 > 1$.

Notice, for example, the deformed energy spectrum (2.42) precisely agrees with the quasilocal energy of the AdS_2 black hole (2.19) upon identifying $\mathcal{E}_0 = \ell M_{\text{ADM}}$ ¹³ together with $L = 2\pi r_B$ and

$$\lambda \equiv \frac{8\pi G_2 \ell^2}{\Phi_r r_B^2}. \quad (2.43)$$

As the Dirichlet wall is pushed to the AdS_2 black hole asymptotic boundary, the flow parameter vanishes. For a one-dimensional quantum mechanical theory, it is more natural to work with the dimensionless quantity¹⁴

$$\mathcal{E} \equiv r_B E(\lambda) = \frac{1}{\lambda} \left(1 - \sqrt{1 - 2\lambda\mathcal{E}_0}\right) = \frac{1}{\lambda} \left(1 - \frac{\tilde{\beta}_T}{\sqrt{\frac{2}{3}\pi^2 c\lambda + \tilde{\beta}_T^2}}\right), \quad (2.44)$$

¹³We rescale the mass since Φ_r is dimensionless to keep λ dimensionless.

¹⁴To arrive at the second equality it is useful to know $r_h = 2\pi\ell r_B / \sqrt{4\pi^2\ell^2 + \beta_T^2}$ and recall energy (2.19).

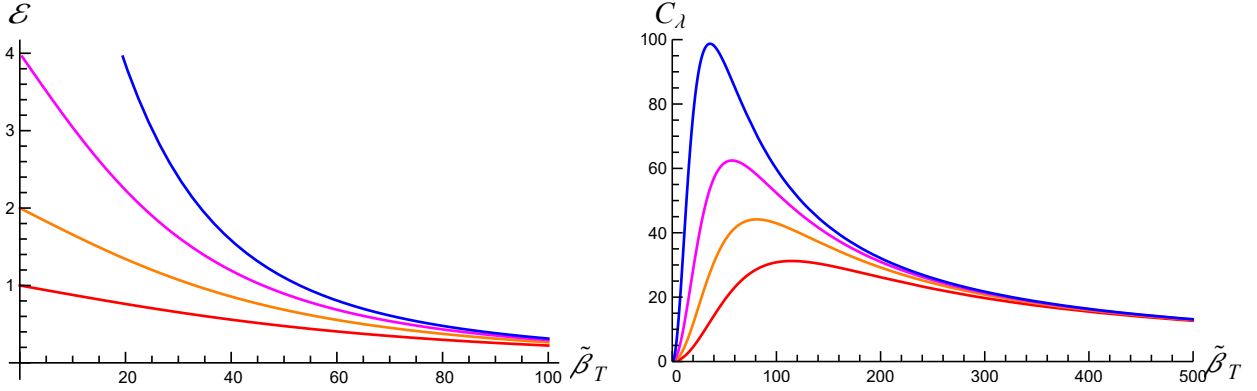


Figure 3: **Left:** Energy levels of the dual theory to AdS₂ JT gravity with a finite cutoff (2.44) at fixed λ (from bottom to top: $\lambda = 1$ (red), $.5$ (orange), $.25$ (magenta), $.1$ (blue)) and $c = 1000$. **Right:** Heat capacity (2.46) at fixed λ for same parameter range.

where $\tilde{\beta}_T \equiv \beta_T/r_B (= \tilde{T}^{-1})$ is the dimensionless (inverse) temperature of the deformed theory, and we defined a constant that is analogous to the central charge in 2D CFTs,

$$\frac{c}{3} \equiv \frac{\Phi_r}{4\pi G_2}. \quad (2.45)$$

At $\lambda = 0$ the energy reduces to $\mathcal{E}(\lambda = 0) = \frac{c}{3}\pi^2\tilde{T}_H^2$, where $\tilde{T}_H = \tilde{T}(\lambda = 0) = T_H\ell$ is the dimensionful boundary temperature of the seed theory. This is identical to the energy-temperature relation for 2D CFTs with c is the central charge, showing the deformed theory in 1D can be understood as the dimensional reduction of the 2D $\overline{\text{T}\overline{\text{T}}}$ deformed theory.

Further, the heat capacity at fixed λ is

$$C_\lambda \equiv -\tilde{\beta}_T^2 \left(\frac{\partial \mathcal{E}(\lambda, \tilde{\beta}_T)}{\partial \tilde{\beta}_T} \right)_\lambda = \frac{1}{\lambda} \frac{\frac{2}{3}\pi^2 c \lambda \tilde{\beta}_T^2}{(\frac{2}{3}\pi^2 c \lambda + \tilde{\beta}_T^2)^{3/2}} = C_{\Phi_B}, \quad (2.46)$$

which is manifestly positive for all real values of $\tilde{\beta}_T$ and $\lambda > 0$. We note that fixing Φ_B in the bulk corresponds to fixing λ in the boundary theory, since $\lambda \propto 1/\Phi_B$. Therefore, the proper data that defines a canonical thermodynamic ensemble in the boundary theory is the (dimensionless) temperature $\tilde{\beta}_T$ and the (dimensionless) deformation parameter λ . Figure 2 displays the energy levels as a function of the flow parameter at fixed \mathcal{E}_0 , and is qualitatively identical to the energy levels of the 2D effective theory dual to AdS₃ gravity with a finite cutoff (see Figure 1 of [33]). However, in the canonical ensemble it is more appropriate to present the microscopic energy levels and corresponding heat capacity as a function of inverse temperature $\tilde{\beta}_T$ at fixed λ (see Figure 3).

2.3 $\overline{\text{T}\overline{\text{T}}}$ deformation for theories dual to general 2D dilaton theories

A more direct computation of the one-dimensional deformed energy spectrum (2.42) – one that is also valid for more general dilaton theories of gravity – can be given by adapting a

proposed generalization of higher-dimensional $\overline{\text{T}\overline{\text{T}}}$ deformations of conformal field theories in a large- N expansion [62] (see also [63]). The idea is the following. Begin by analyzing the Hamiltonian constraint of the bulk theory, e.g., the general dilaton gravity theory (2.1), which is in part given in terms of components of the quasi-local Brown-York stress-tensor. From the Hamiltonian constraint, one defines a bulk flow equation for the on-shell dilaton gravity action. Assuming the standard holographic dictionary holds for a bulk gravity theory with Dirichlet boundary conditions at a finite timelike wall, the bulk flow equation then *defines* the flow equation of the effective one-dimensional quantum mechanical theory, I_{EFT} . One is consequently led to the following flow equation [40] (see Appendix A for details)

$$\partial_\lambda I_{\text{EFT}} = \int d\tau \sqrt{\gamma} \left[\frac{(T_\tau^\tau)^2 - (\ell\lambda)^{-2} \left(1 - \frac{\ell^2}{2\Phi_r} \sqrt{\frac{c\lambda}{6}} V\left(\Phi_r \sqrt{\frac{6}{c\lambda}}\right) \right)}{2\ell^{-1} - 2\lambda T_\tau^\tau} \right], \quad (2.47)$$

where we have introduced the parameter $c \equiv \frac{3\Phi_r}{4\pi G_2}$. Writing $T_\tau^\tau = E(\lambda)$, the flow equation characterizing the deformed energy spectrum $E(\lambda)$ is

$$\partial_\lambda E = \frac{E^2 - (\ell\lambda)^{-2} \left(1 - \frac{\ell^2}{2\Phi_r} \sqrt{\frac{c\lambda}{6}} V\left(\Phi_r \sqrt{\frac{6}{c\lambda}}\right) \right)}{2\ell^{-1} - 2\lambda E}, \quad (2.48)$$

with a generic solution for $\mathcal{E}(\lambda) = r_B E(\lambda)$,

$$\mathcal{E}(\lambda) = \frac{1}{\lambda} \left(1 \pm \sqrt{C_1 \lambda + \lambda \frac{c}{6} f\left(\Phi_r \sqrt{\frac{6}{c\lambda}}\right)} \right), \quad (2.49)$$

for integration constant C_1 and where

$$f(x) \equiv \frac{\ell^2}{\Phi_r^2} \int^x V(y) dy. \quad (2.50)$$

Notice the choice in ‘ \pm ’ in front of the square root in (2.49) leads to two different solutions. For example, consider the ‘ $-$ ’ branch. Then, imposing the initial data $\mathcal{E}(\lambda = 0) \equiv \mathcal{E}_0$ fixes $C_1 = -2\mathcal{E}_0$, from which we find agreement with the energy spectrum (2.44) dual to the AdS₂ JT black hole when $V(\Phi) = 2\Phi/\ell^2$. Moreover, the choice of sign ‘ \pm ’ also allows for matching to the quasi-local energies (2.26) of the cosmological (+) or black hole (−) patch in dS₂ JT gravity. Indeed, for $V(\Phi) = -2\Phi/\ell^2$, and setting $C_1 \equiv 2\mathcal{E}_H$, Eq. (2.49) yields

$$\mathcal{E}^{c,h}(\lambda, \mathcal{E}_H) = \frac{1}{\lambda} \left(1 \pm \sqrt{2\lambda \mathcal{E}_H - 1} \right) = \frac{1}{\lambda} \left(1 \pm \frac{\tilde{\beta}_T}{\sqrt{\frac{2}{3}\pi^2 c\lambda - \tilde{\beta}_T^2}} \right), \quad (2.51)$$

where ‘ $+$ ’ refers to the cosmological patch and ‘ $-$ ’ to the black hole patch. Using the λ identification (2.43) and $\mathcal{E}_H \equiv \ell M_{\text{ADM}}^{\text{dS}_2} = \frac{\Phi_r r_H^2}{16\pi G_2 \ell^2}$, we recover the dS₂ quasi-local energy energies (2.26), with $\mathcal{E}^{c,h}(\lambda) = |r_B| E_{\text{BY}}^{c,h}$. Notice that the range of λ is restricted to $[\frac{1}{2\mathcal{E}_H}, \infty]$,

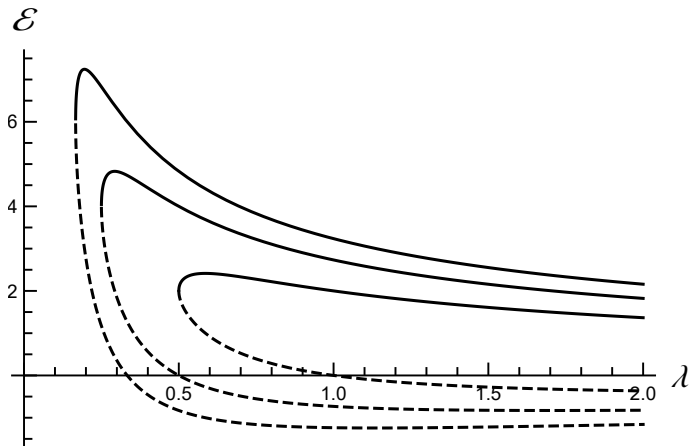


Figure 4: Energy levels \mathcal{E} of the dual theory to dS_2 JT gravity with a timelike Dirichlet boundary as a function of λ at fixed \mathcal{E}_H (2.51) (from left to right: $\mathcal{E}_H = 3, 2, 1$). Solid (dashed) lines indicate energy levels of the cosmic (black hole) patch.

where the lower bound corresponds to the situation in the bulk where the system boundary coincides with the horizon, $r_B = r_h$.

The heat capacity (2.46) for the quantum mechanical system dual to dS_2 JT gravity is

$$C_\lambda^{c,h} = \mp \frac{1}{\lambda} \frac{\frac{2}{3}\pi^2 c \lambda \tilde{\beta}_T^2}{\left(\frac{2}{3}\pi^2 c \lambda - \tilde{\beta}_T^2\right)^{3/2}}, \quad (2.52)$$

with $-$ ($+$) for the cosmic (black hole) patch. Figure 4 displays the microscopic energy spectrum (2.51) as a function of λ at fixed \mathcal{E}_H , and Figure 5 portrays the microscopic energy and heat capacity as functions of $\tilde{\beta}_T = \beta_T/r_B$ at fixed λ . Crucially, the system that is dual to the cosmic patch is thermally unstable, while the system that is dual to the black hole patch is stable against thermal fluctuations. As is well known from standard statistical mechanics, negative heat capacity implies the canonical ensemble partition function for the cosmological horizon patch (for bulk or boundary theory) is ill-defined. More precisely, positivity of heat capacity is linked to the convergence of the integral representation of the canonical partition function in a steepest descents approximation (see, e.g., [64]).

2.4 Cardy-like formulae for the thermal entropy of the dual deformed theory

At fixed λ the (dimensionless) energy of the deformed boundary theory should satisfy the first law

$$d\mathcal{E} = \tilde{T}dS \quad \text{at fixed } \lambda, \quad (2.53)$$

where $\tilde{T} = \tilde{\beta}_T^{-1}$ is the dimensionless boundary temperature. We can derive the thermal entropy S (up to a constant) by integrating the first law. In the canonical ensemble (at fixed

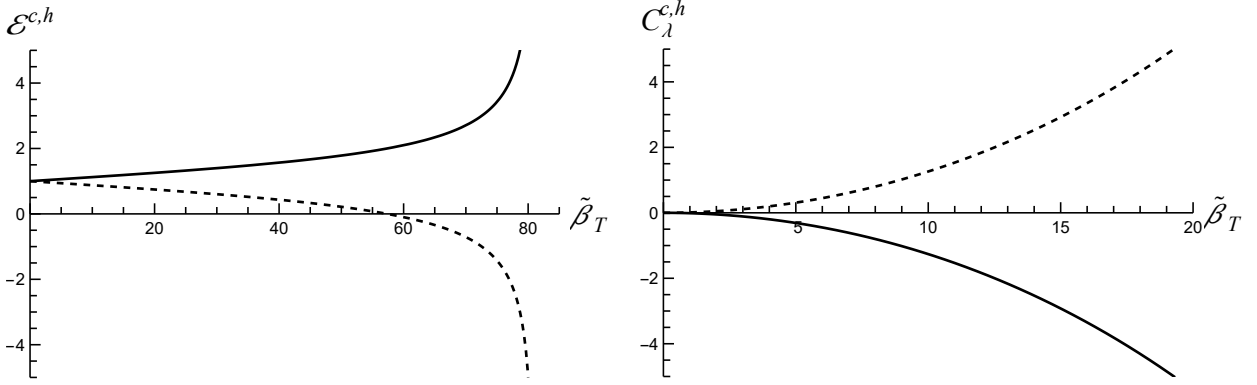


Figure 5: Left: Microscopic energy of the dual theory to dS_2 JT gravity with a timelike Dirichlet boundary (2.51) at fixed $\lambda = 1$, and $c = 1000$. Solid (dashed) curve denotes cosmic (black hole) horizon patch. **Right:** Heat capacity (2.52) for same parameter range.

\tilde{T}) it follows from the final expressions in energies (2.44) and (2.51) that the entropy takes the form

$$\text{for thermal states dual to AdS}_2: \quad S(\lambda, \tilde{\beta}_T) = S_0 + \frac{\frac{2}{3}\pi^2 c}{\sqrt{\frac{2}{3}\pi^2 c \lambda + \tilde{\beta}_T^2}}, \quad (2.54)$$

$$\text{for thermal states dual to dS}_2: \quad S(\lambda, \tilde{\beta}_T) = S_0 \pm \frac{\frac{2}{3}\pi^2 c}{\sqrt{\frac{2}{3}\pi^2 c \lambda - \tilde{\beta}_T^2}}, \quad (2.55)$$

where ‘+’ refers to states dual to the cosmological patch, and ‘-’ to states dual to the black hole patch in dS_2 .

For thermal states dual to AdS_2 , the entropy of the undeformed theory is

$$S(\lambda = 0) = S_0 + \frac{2}{3}\pi^2 c \tilde{T}_H, \quad (2.56)$$

where $\tilde{T}_H = \tilde{T}(\lambda = 0) = T_H \ell$ is the dimensionless undeformed boundary temperature. This entropy agrees (up to a constant) with the Cardy formula for the canonical entropy in 2D CFTs with equal left- and right-moving energies and central charges. The formulae above are extensions of the canonical Cardy entropy to finite λ and, in fact, they also hold for $\overline{\text{T}\overline{\text{T}}}$ deformations of 2D CFTs. Moreover, for thermal states dual to dS_2 there is a minimum value for $\lambda \tilde{T}^2$, given by $1/(\frac{2}{3}\pi^2 c)$.

In the microcanonical ensemble (at fixed \mathcal{E}), on the other hand, the entropy for finite λ is given by

$$\text{for thermal states dual to AdS}_2: \quad S(\lambda, \mathcal{E}) = S_0 + 2\pi \sqrt{\frac{c}{6} \mathcal{E} (2 - \lambda \mathcal{E})}, \quad (2.57)$$

$$\text{for thermal states dual to dS}_2: \quad S(\lambda, \mathcal{E}) = S_0 \pm 2\pi \sqrt{\frac{c}{6} \left(\mathcal{E} (\lambda \mathcal{E} - 2) + \frac{2}{\lambda} \right)}. \quad (2.58)$$

For states dual to AdS₂ the range of the deformation parameter is from $\lambda = 0$ to $\lambda = 1/\mathcal{E}$, where the lower bound corresponds to $r_B = \infty$ in the bulk and the upper bound to $r_B = r_H$. For states dual to dS₂ the range is from $\lambda = 1/\mathcal{E}$ to $\lambda = \infty$, where the lower bound is dual to $r_B = r_h$ in the bulk and the upper bound to $r_B = 0$. For the undeformed theory, the microcanonical entropy of thermal states dual to AdS₂ reduces to

$$S(\lambda = 0, \mathcal{E}) = S_0 + 2\pi\sqrt{\frac{c}{3}\mathcal{E}_0}, \quad (2.59)$$

which coincides (up to a constant) with the well-known Cardy formula for microcanonical entropy in 2D CFTs when the left- and right-moving energies are the same [39, 65]. This further confirms the boundary holographic theory in 1D can indeed be viewed as a dimensional reduction of a 2D CFT. It is also noteworthy that the microcanonical entropy reduces to the Cardy formula for $\lambda = 1/\mathcal{E} = 1/(2\mathcal{E}_0)$, which corresponds to the setup where the Dirichlet wall is located at the horizon.

The negative heat capacity of the cosmic patch, and hence thermal instability, can be further seen from the microcanonical entropy (2.58). It is straightforward to verify the entropy associated to the cosmic horizon patch is a *convex* function of energy \mathcal{E} , a common characteristic of an unstable thermal system. Convexity of the entropy coincides with the canonical partition function diverging in a steepest descent approximation (cf. [64]). In contrast, entropy for the black hole horizon patch, or states dual to AdS₂ are *concave* in the deformed energy, coinciding with thermal stability.

Finally, both the canonical and microcanonical entropy of the deformed boundary theory match exactly with the Bekenstein-Hawking entropy (2.13) for 2D dilaton gravity in the bulk,

$$S_{\text{BH}} = \frac{\Phi_0}{4G_2} + \frac{\Phi_h}{4G_2}, \quad (2.60)$$

upon identifying $\Phi_0/4G_2$ with the constant term S_0 in the boundary entropy formulae (2.54)-(2.58) and $\Phi_h/4G_2$ with the second term in these formulae. This can be checked explicitly using the holographic dictionary for λ and c , (2.43) and (2.45) respectively, and inserting the expressions for the temperatures and energies in the previous sections.

We observe that the thermal entropy is independent of λ in an ensemble of fixed \mathcal{E}_0 , i.e., the number of states does not change if we fix \mathcal{E}_0 . In the bulk, fixing \mathcal{E}_0 amounts to fixing the ADM mass. For any λ the Bekenstein-Hawking entropy matches with the Cardy entropy $S = 2\pi\sqrt{c\mathcal{E}_0/3}$, and is clearly independent of λ . Alternatively, if \mathcal{E} or $\tilde{\beta}$ are held fixed instead of \mathcal{E}_0 , then the entropy clearly does depend on λ . Note that \mathcal{E} and $\tilde{\beta}$ are the thermodynamic variables of the deformed theory, whereas \mathcal{E}_0 is the energy of the undeformed theory. Thus, whether the entropy is a function of the deformation parameter λ depends on the ensemble, but for the ensemble that fixes the thermodynamic variables of the deformed theory itself (e.g., \mathcal{E} or $\tilde{\beta}$) the entropy is indeed a function of λ .

3 Interpolating geometries via $T\bar{T}$ deformations

In the previous section we reviewed a general class of dilaton gravity theories with a timelike Dirichlet boundary that has a dual description in terms of a one-dimensional $T\bar{T}$ deformed quantum mechanical theory [40, 43]. Evidence for this comes from the equivalence of the microscopic deformed energy spectrum and the quasi-local energy of the gravitational theory. Notably, we found the generic solution to the microscopic flow equation is capable of describing either the cosmological or black hole horizon patch in dS_2 JT gravity, giving a microscopic perspective of quasi-local energy in dS_2 , and consequently, the entropy.

An interesting class of dilaton gravity models to consider are those which interpolate between dS_2 and AdS_2 spaces [19, 22, 66, 67]. The simplest such set-up is dubbed the “centaur geometry” [22], having a dS_2 interior but AdS_2 asymptotics. Motivation for these dilaton models is that they provide a natural setting to develop dS_2 (static patch) holography, where the dS static patch is accessible to probe from the asymptotic AdS boundary.¹⁵ Here we apply the $T\bar{T}$ formalism of the previous section to explicitly develop a microscopic picture of the centaur model (such an analysis was alluded to in [40] but not developed).

3.1 Centaur (A) dS_2 geometries

There are two different centaur geometries: one where the interior dS_2 space includes the cosmological horizon, and another where dS_2 space with a black hole horizon, both glued to an AdS_2 exterior geometry. In the former, the dilaton decreases towards the boundary, and in the latter the dilaton increases towards the boundary. Like in the previous sections, we associate a positive value of the dilaton to the cosmological horizon, and a negative value to the black hole horizon, following our convention in [17].¹⁶

The centaur geometry can be obtained as a solution of a two-dimensional dilaton-gravity theory (2.1) for an array of potentials $V(\Phi)$. For concreteness, we take

$$V(\Phi) = \mp \frac{2}{\ell^2} |\Phi|. \tag{3.1}$$

For this dilaton potential the centaur geometries are described by the solution (2.6), where the blackening factor is, respectively, given by

$$(a) \text{ centaur with cosmological horizon: } N(r) = \begin{cases} \frac{r_H^2 - r^2}{\ell^2}, & r_H \geq r \geq 0, \\ \frac{r_H^2 + r^2}{\ell^2}, & 0 \geq r \geq -\infty, \end{cases} \tag{3.2}$$

$$(b) \text{ centaur with black hole horizon: } N(r) = \begin{cases} \frac{r_H^2 - r^2}{\ell^2}, & -r_H \leq r \leq 0, \\ \frac{r_H^2 + r^2}{\ell^2}, & 0 \leq r \leq \infty. \end{cases} \tag{3.3}$$

¹⁵There is a no-go theorem [68] which states dS_{d+1} geometries glued to asymptotically AdS_{d+1} space for $d > 1$ will be hidden behind the black hole horizon of the asymptotically AdS_{d+1} . The $d = 1$ interpolating geometries evade this theorem.

¹⁶This is different from the convention in the original work [22], where the dilaton is taken to be negative near the cosmological horizon, and positive near the black hole horizon.

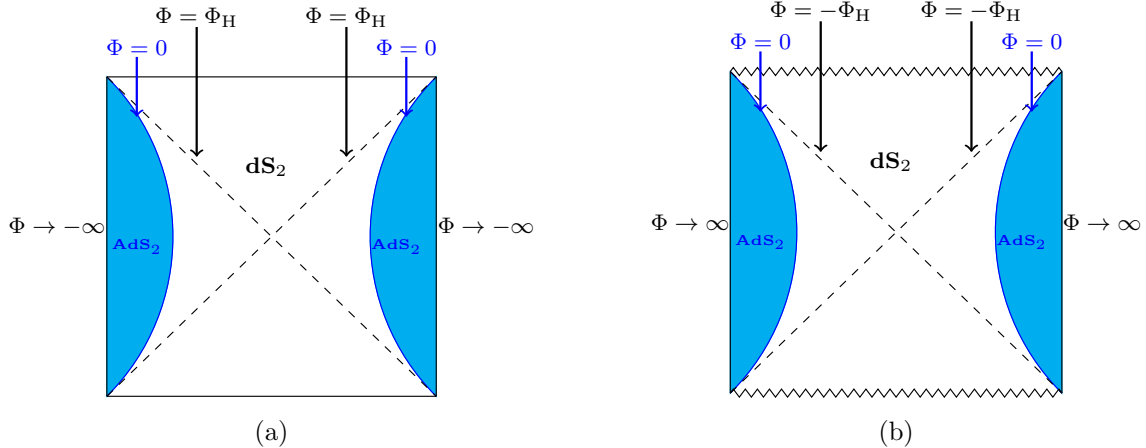


Figure 6: Penrose diagram of centaur geometry, interpolating between the dS_2 space (white) and AdS_2 space (blue). (a) Centaur geometry with a cosmological horizon. In this case the dilaton is positive on the horizon and decreases towards the boundary, where it becomes minus infinity. (b) Centaur geometry with a black hole horizon. The dilaton is negative at the horizon and increases towards to the AdS boundary, where it diverges.

The minus sign in the potential (3.1) yields a centaur solution with a dS_2 cosmological horizon (at $r = r_H$), and the plus sign corresponds to a centaur geometry with a black hole horizon (at $r = -r_H$). In the former case, the region $r > 0$ describes dS_2 space, and the region $r < 0$ corresponds to a global AdS_2 patch. In the latter case, on the other hand, the region with $r < 0$ corresponds to dS_2 , and the region with $r > 0$ to global AdS_2 . In both cases the interface between AdS_2 and dS_2 is located at $r = 0$. The Penrose diagrams of the two centaur geometries are displayed in Figure 6.

Notice in the former case the dilaton $\Phi = \Phi_r r / \ell$ is positive at the cosmological horizon and decreases towards the AdS boundary, where it becomes minus infinity. In contrast, in the latter case the dilaton is negative at the black hole horizon and increases monotonically towards the AdS boundary, where it blows up. Since $\Phi_0 + \Phi$ can be interpreted as the inverse of the gravitational coupling, $\Phi \rightarrow +\infty$ corresponds to a weak gravitating regime and $\Phi \rightarrow -\infty$ to a strongly gravitating regime (since $\Phi_0 + \Phi \rightarrow 0$ in that case). Hence, in the presence of a cosmological horizon the semiclassical description of the boundary of the centaur geometry breaks down. Therefore, it is not possible to define a seed (undeformed) dual quantum mechanical theory at the boundary of a centaur geometry with a cosmological horizon. Perhaps it is possible to remedy this issue by defining the seed theory at a cutoff surface away from the boundary. Putting this issue aside, below we will compare the energy spectra and heat capacities of the $T\bar{T}$ deformed theories dual the two centaur models.

Next, we introduce a timelike Dirichlet boundary with a fixed dilaton $\Phi_B \propto r_B$ and a

fixed temperature, whose inverse value is on shell given by the inverse Tolman temperature

$$(a) \text{ centaur with cosmological horizon: } \beta_{\text{T}} = \begin{cases} \frac{\beta_{\text{H}}}{\ell} \sqrt{r_{\text{H}}^2 - r_{\text{B}}^2}, & r_{\text{H}} \geq r_{\text{B}} \geq 0, \\ \frac{\beta_{\text{H}}}{\ell} \sqrt{r_{\text{H}}^2 + r_{\text{B}}^2}, & 0 \geq r_{\text{B}} \geq -\infty, \end{cases} \quad (3.4)$$

$$(b) \text{ centaur with black hole horizon: } \beta_{\text{T}} = \begin{cases} \frac{\beta_{\text{H}}}{\ell} \sqrt{r_{\text{H}}^2 - r_{\text{B}}^2}, & -r_{\text{H}} \leq r_{\text{B}} \leq 0, \\ \frac{\beta_{\text{H}}}{\ell} \sqrt{r_{\text{H}}^2 + r_{\text{B}}^2}, & 0 \leq r_{\text{B}} \leq \infty, \end{cases} \quad (3.5)$$

where $\beta_{\text{H}} = 2\pi\ell^2/r_{\text{H}}$. In both centaur geometries, the inverse temperatures range from $[0, 2\pi\ell]$ in the dS region, and $[2\pi\ell, \infty]$ in the AdS patch.

Additionally, the quasi-local energy at an arbitrary Dirichlet wall is given on shell by

$$E_{\text{BY}} = \begin{cases} \frac{1}{8\pi G_2 \ell} \left(\Phi_B \pm \frac{|\Phi_B| \beta_{\text{T}}}{\sqrt{4\pi^2 \ell^2 - \beta_{\text{T}}^2}} \right), & 0 \leq \beta_{\text{T}} \leq 2\pi\ell, \\ \frac{1}{8\pi G_2 \ell} \left(\Phi_B \pm \frac{|\Phi_B| \beta_{\text{T}}}{\sqrt{\beta_{\text{T}}^2 - 4\pi^2 \ell^2}} \right), & 2\pi\ell \leq \beta_{\text{T}} < \infty, \end{cases} \quad (3.6)$$

where the plus sign corresponds to a centaur geometry with a cosmological horizon, and the minus sign corresponds to a geometry with a dS₂ black hole horizon. Note that for the ‘cosmological’ centaur the Brown-York energy diverges to plus infinity at the interface where $\beta_{\text{T}} = 2\pi\ell$, whereas for the ‘black hole’ centaur the Brown-York energy diverges to minus infinity at the interface and it goes to zero at the AdS boundary. Interestingly, upon multiplying the quasi-local energy with $\sqrt{N(r_{\text{B}})}$ and taking the limit $r_{\text{B}} \rightarrow \mp\infty$ (or $\beta_{\text{T}} \rightarrow \infty$) we find that the ADM mass of the centaur geometry is negative in the presence of a black hole horizon and positive in the presence of a cosmological horizon

$$M_{\text{ADM}}^{\text{cent}} = \pm \frac{\Phi_r r_{\text{H}}^2}{16\pi G_2 \ell^3}. \quad (3.7)$$

3.2 Thermodynamics of the dual deformed theory

We want to find the energy spectrum of the deformed dual microscopic theory. We can apply the previous general solutions of the flow equation (2.48) to the particular centaur dilaton potential in (3.1) to derive for the energy spectrum. For the dS region of the centaur geometry the deformed energies are given by (2.51). For the AdS region we fix the constant in (2.49) to be $C_1 = 2\mathcal{E}_H$. The deformed energy spectrum for the centaur model thus takes the form, as a function of the dimensionless boundary temperature $\tilde{\beta}_{\text{T}} = \beta_{\text{T}}/r_{\text{B}}$,

$$\mathcal{E}(\lambda, \tilde{\beta}_{\text{T}}) = \begin{cases} \frac{1}{\lambda} \left(1 \pm \frac{\tilde{\beta}_{\text{T}}}{\sqrt{\frac{2}{3}\pi^2 c\lambda - \tilde{\beta}_{\text{T}}^2}} \right), & 0 \leq \tilde{\beta}_{\text{T}}^2 \leq \frac{2}{3}\pi^2 c\lambda, \\ \frac{1}{\lambda} \left(1 \pm \frac{\tilde{\beta}_{\text{T}}}{\sqrt{\tilde{\beta}_{\text{T}}^2 - \frac{2}{3}\pi^2 c\lambda}} \right), & \frac{2}{3}\pi^2 c\lambda \leq \tilde{\beta}_{\text{T}}^2 < \infty, \end{cases} \quad (3.8)$$

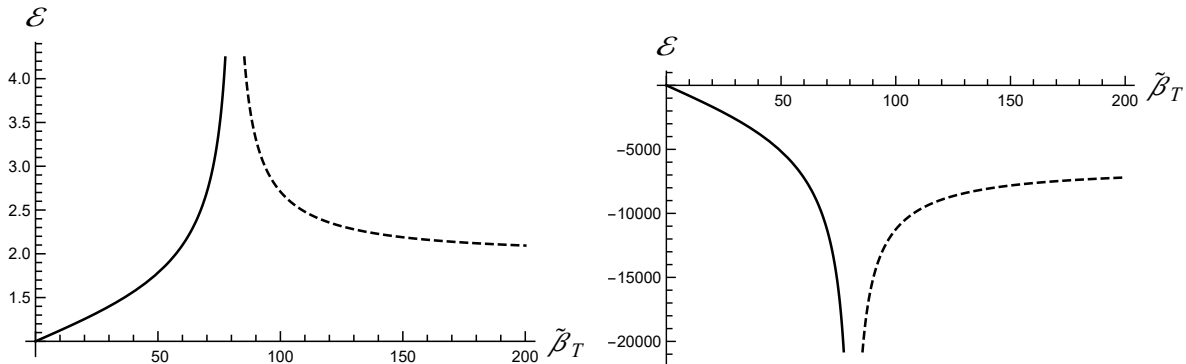


Figure 7: Energy spectrum (3.8) as a function of $\tilde{\beta}_T$ for $\lambda = 1$ and $c = 1000$ for the microscopic theory dual to the centaur model in the presence of (a) a cosmological horizon, and (b) a black hole horizon. The solid line represents the region $\tilde{\beta}_T^2 \leq \frac{2}{3}\pi^2 c\lambda$, and the dashed line for $\tilde{\beta}_T^2 \geq \frac{2}{3}\pi^2 c\lambda$.

or, as a function of \mathcal{E}_H ,

$$\mathcal{E}(\lambda, \mathcal{E}_H) = \begin{cases} \frac{1}{\lambda} (1 \pm \sqrt{2\lambda\mathcal{E}_H - 1}) , & \frac{1}{2\mathcal{E}_H} \leq \lambda \leq \infty , \\ \frac{1}{\lambda} (1 \pm \sqrt{2\lambda\mathcal{E}_H + 1}) , & 0 \leq \lambda \leq \infty . \end{cases} \quad (3.9)$$

The upper expression after the curly bracket corresponds to states dual to dS_2 , whereas the lower expressions are for states dual to AdS_2 . Moreover, the plus sign corresponds to a centaur geometry with a cosmological horizon, and the minus sign holds for states dual to a centaur geometry with a dS_2 black hole horizon. This energy spectrum agrees with the Brown-York energy (3.6) if we identify $\mathcal{E} = |r_B|E_{BY}$ and $\mathcal{E}_H \equiv \Phi_r r_H^2 / (16\pi G_2 \ell^2)$. The energy spectra for the deformed theories are shown in Figures 7 and 8, for theories dual to cosmological centaur models and black hole centaur models. Note at the interface between the dS and AdS regions, at fixed \mathcal{E}_H the energy goes to zero as $\lambda \rightarrow \infty$, but at fixed λ the energy diverges at the interface.

By integrating the first law (2.53) at fixed λ we can derive the thermal entropy for states dual to the centaur geometry (3.8). For the canonical ensemble, we find

$$S(\lambda, \tilde{\beta}_T) = \begin{cases} S_0 \pm \frac{\frac{2}{3}\pi^2 c}{\sqrt{\frac{2}{3}\pi^2 c\lambda - \tilde{\beta}_T^2}} , & \tilde{\beta}_T \leq \sqrt{\frac{3}{2\pi^2 c\lambda}} , \\ S_0 \pm \frac{\frac{2}{3}\pi^2 c}{\sqrt{\tilde{\beta}_T^2 - \frac{2}{3}\pi^2 c\lambda}} , & \tilde{\beta}_T \geq \sqrt{\frac{3}{2\pi^2 c\lambda}} , \end{cases} \quad (3.10)$$

where the upper expression corresponds to the case where the boundary (on which the microscopic theory lives) is located in the dS_2 region, and for the lower expression the Dirichlet wall is located in the (global) AdS_2 region of the centaur geometry. We note that the upper expression for the entropy agrees with (2.55), but the lower expression differs from (2.54) since the AdS_2 region in the centaur geometry corresponds to global AdS , whereas the AdS_2

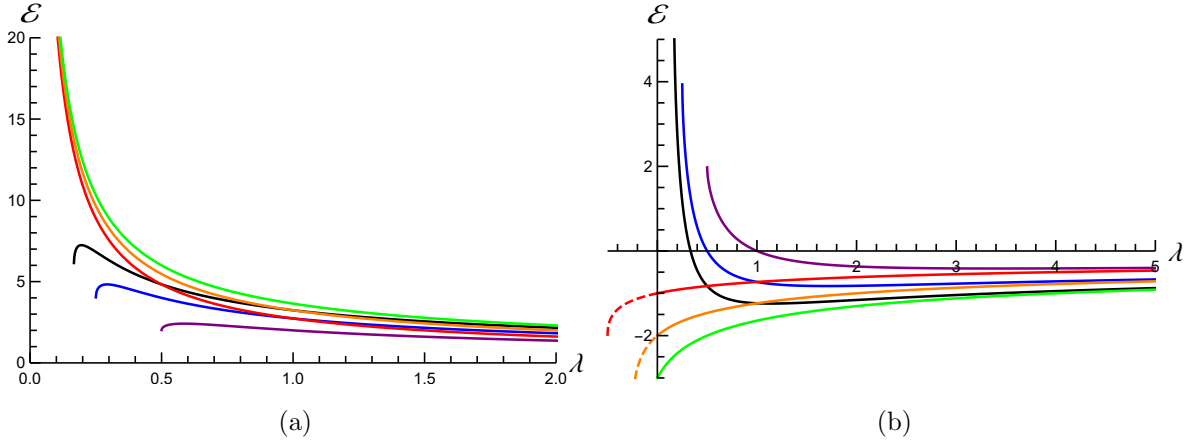


Figure 8: The energy spectrum (3.9) of the centaur model for different representative values of \mathcal{E}_H in the presence of (a) a dS_2 cosmological horizon, and (b) a dS_2 black hole horizon. Like in Figure 2, we have allowed for an analytic continuation for the deformation parameter $\lambda = -\frac{1}{2\mathcal{E}_H}$ in the global AdS_2 region (dashed lines), corresponding to the lower line in (3.9); while the upper line corresponds to the dS_2 region. Purple, blue and black solid lines indicate $\mathcal{E}_H = 1, 2, 3$ respectively in the dS_2 region; while red, orange and green correspond to $\mathcal{E}_H = 1, 2, 3$ in the AdS_2 region.

region considered in (2.54) corresponds to an eternal AdS_2 black hole (or Rindler- AdS). This is related to the fact that the temperature in the AdS_2 region here is bounded above (at fixed λ), whereas in the case considered in (2.54) it is unbounded above.

The microcanonical entropy of thermal states dual to the centaur geometry is

$$\text{For states dual to the } \text{dS}_2 \text{ region: } S(\lambda, \mathcal{E}) = S_0 \pm 2\pi \sqrt{\frac{c}{6} \left(\mathcal{E}(\lambda\mathcal{E} - 2) + \frac{2}{\lambda} \right)}, \quad (3.11)$$

$$\text{For states dual to the } \text{AdS}_2 \text{ region: } S(\lambda, \mathcal{E}) = S_0 \pm 2\pi \sqrt{\frac{c}{6} \mathcal{E}(\lambda\mathcal{E} - 2)}. \quad (3.12)$$

Note that the entropy diverges at the interface $\lambda = \infty$ ($r_B = 0$) between the AdS_2 and dS_2 patches. Again, the microcanonical entropy for thermal states dual to a (global) AdS_2 region differs slightly from (2.57).

Furthermore, the heat capacity at fixed λ can be easily computed from the energy spectrum, using the definition in (2.46),

$$C_\lambda = \begin{cases} \mp \frac{1}{\lambda} \frac{\frac{2}{3}\pi^2 c \lambda \tilde{\beta}_T^2}{(\frac{2}{3}\pi^2 c \lambda - \tilde{\beta}_T^2)^{3/2}}, & 0 \leq \tilde{\beta}_T^2 \leq \frac{2}{3}\pi^2 c \lambda, \\ \pm \frac{1}{\lambda} \frac{\frac{2}{3}\pi^2 c \lambda \tilde{\beta}_T^2}{(\tilde{\beta}_T^2 - \frac{2}{3}\pi^2 c \lambda)^{3/2}}, & \tilde{\beta}_T^2 \geq \frac{2}{3}\pi^2 c \lambda, \end{cases} \quad (3.13)$$

where the upper sign corresponds to the ‘cosmological’ centaur model and the lower sign to the ‘black hole’ centaur model. The heat capacity at fixed λ as a function of the $\tilde{\beta}_T$ is shown

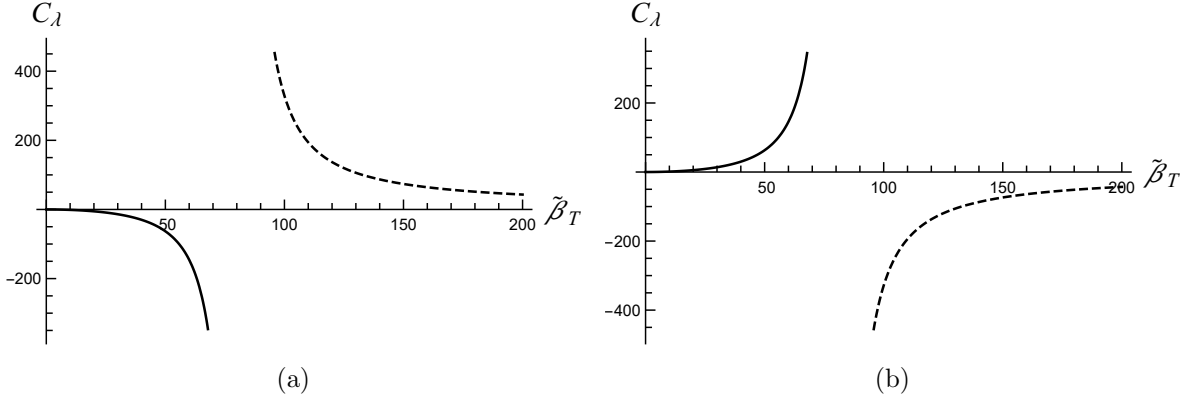


Figure 9: Heat capacity of the centaur model with (a) a cosmological horizon, corresponding to the upper sign in (3.13), and (b) a black hole horizon, i.e. the lower sign in (3.13). The solid line represents the region $0 \leq \tilde{\beta}_T \leq \frac{2}{3}\pi^2 c\lambda$, and the dashed line for $\tilde{\beta}_T \geq \frac{2}{3}\pi^2 c\lambda$. We have set $c = 1000$ and $\lambda = 1$ in the plots.

in Figure 9. We emphasize that the heat capacity switches sign for both centaur models from the dS region to the AdS region. This is a distinctive feature of deformed microscopic theories dual to the centaur geometry, since for instance for theories dual to AdS₂ JT gravity the heat capacity is positive for all temperatures, see (2.46). It is further interesting to note that the heat capacity also depends on the nature of the horizon, i.e. the signs in the heat capacity are precisely opposite for the ‘cosmological’ and ‘black hole’ centaur models. It is especially interesting that for microscopic theories that live on a Dirichlet wall inside the AdS region the heat capacity is positive in the presence of a cosmological horizon and negative in the presence of a dS₂ black hole horizon. This can again be contrasted to the heat capacity of an AdS₂ black hole horizon, which is always positive. Thus, the heat capacity is a useful observable to distinguish the microscopic dual theory of the centaur geometry from the dual theory of AdS₂ space.

4 Dilaton gravity from $T\bar{T} + \Lambda_2$

Above we provided a holographic interpretation of quasi-local thermodynamics of the centaur model via $T\bar{T}$ deformations. Here we derive the two-dimensional analog of $T\bar{T} + \Lambda_2$ deformations [25, 26, 28, 35, 69],¹⁷ originally used to connect patches of dS₃ to AdS₃ and provide a microstate counting of dS₃ entropy. This is accomplished by first generalizing $T\bar{T} + \Lambda_2$ flows to connect more general (A)dS₃ patches, namely BTZ and Schwarzschild-dS₃ of the same mass. Notably, the resulting deformed energy spectrum maps each original energy level (where $\lambda = 0$) to different values of λ . That is, there is not a single theory, at a given value of λ , which has all of these energy levels as part of its spectrum; the flow we consider is

¹⁷See [70] for recent developments on $T^2 + \Lambda_3$ deformations.

tuned such that only one of the states looks like Schwarzschild-dS₃ from a particular value λ_0 onwards. We then dimensionally reduce these more general flows, and show they can be used to holographically describe AdS₂ to a dS₂ region characterized by an appropriate dilaton-gravity theory. We will see the microscopic energy spectrum and quasi-local thermodynamics are compatible with a $\text{T}\bar{\text{T}}$ -deformation of the quantum theory dual to the centaur geometry.

4.1 Review of $\text{T}\bar{\text{T}} + \Lambda_2$ deformations and patchwise holography

We begin with a brief review of solvable irrelevant $\text{T}\bar{\text{T}} + \Lambda_2$ flows and how they holographically correspond to connecting an AdS₃ patch to a dS₃ patch. We extend this to more general (A)dS₃ patches in the subsequent section before deriving its two-dimensional analog via dimensional reduction.

On the field theory side, to accommodate a dS₃ region, the idea is to slightly modify the 1-parameter family of deformed theories (2.30) by including a two-dimensional ‘cosmological constant’ Λ_2 [35, 69]

$$I_{\text{QFT}} = I_{\text{CFT}} + \mu \int d^2x \sqrt{\gamma} \text{T}\bar{\text{T}} + \frac{(1-\eta)}{\mu} \int d^2x \sqrt{\gamma}. \quad (4.1)$$

Here $\eta = \pm 1$, where $\eta = +1$ returns the standard $\text{T}\bar{\text{T}}$ deformed theory. The associated flow equation is

$$\partial_\mu \log Z_{\text{QFT}}(\mu, \eta) = - \int d^2x \sqrt{\gamma} \langle \text{T}\bar{\text{T}} \rangle + \frac{(1-\eta)}{\mu^2} \int d^2x \sqrt{\gamma}, \quad (4.2)$$

together with the initial condition $Z_{\text{QFT}}(\mu = 0, \eta = 1) = Z_{\text{CFT}}$. The Burgers equation (2.37) defining the microscopic energy spectrum $\mathcal{E}_n(\lambda)$ becomes (see Appendix A of [35])¹⁸

$$4\pi \partial_\lambda \mathcal{E}_n - 2\lambda \mathcal{E}_n \partial_\lambda \mathcal{E}_n - \mathcal{E}_n^2 + P_n^2 L^2 + \left(\frac{2\pi}{\lambda}\right)^2 (1-\eta) = 0. \quad (4.3)$$

where λ is defined in (2.36). The general solution yields

$$E_n(\lambda, \eta) = \frac{2\pi}{\lambda L} \left(1 \pm \sqrt{\eta - \frac{4C_1\lambda}{2\pi^2} + \lambda^2 J_n^2} \right), \quad (4.4)$$

where recall $\mathcal{E}_n = E_n L$. How the integration constant C_1 and which \pm branch are determined will be described momentarily.

A key insight of [35] is that the flow equation (4.2) serves as a prescription that is to be applied piecewise. Specifically, the total flow trajectory is comprised of two legs: (i) start with a pure $\text{T}\bar{\text{T}}$ deformation (where $\eta = 1$), flowing from $\lambda = 0$ to some positive constant $\lambda = \lambda_0$, then (ii) at $\lambda = \lambda_0$, turn on $\eta = -1$, thus connecting the pure $\text{T}\bar{\text{T}}$ segment of the trajectory to a $\text{T}\bar{\text{T}} + \Lambda_2$ segment.¹⁹ For special values of λ_0 , the combined flow dualizes to

¹⁸To compare, note the dimensionless flow parameter y in [35] is related to ours via $2\pi^2 y_{\text{there}} = \lambda_{\text{here}}$.

¹⁹The two segments are connected by imposing the general boundary condition $Z_{\text{QFT}}(\lambda = \lambda_0, \eta = -1) = Z_{\text{QFT}}(\lambda = \lambda_0, \eta = 1)$.

sewing together gravitating patches of AdS₃ to dS₃ space [25, 26, 35]. To see how this works, consider three-dimensional Einstein gravity with cosmological constant $2\Lambda_3 = -\frac{2\eta}{\ell_3^2}$, and a Gibbons-Hawking-York boundary term plus a local counterterm

$$I_{\text{EH}} = \frac{1}{16\pi G_3} \int_{\mathcal{M}} d^3x \sqrt{-g} \left(R + \frac{2\eta}{\ell_3^2} \right) + \frac{1}{8\pi G_3} \int_{\partial\mathcal{M}} d^2x \sqrt{h} \left(K - \frac{1}{\ell_3} \right). \quad (4.5)$$

Clearly, a flow between $\eta = +1$ to $\eta = -1$ corresponds to a transition from bulk spacetimes with $\Lambda_3 < 0$ to those with $\Lambda_3 > 0$, e.g., the BTZ black hole and dS₃. The goal is to smoothly connect a patch of AdS₃ to a patch of dS₃, particularly one which contains the dS₃ cosmological horizon, whilst respecting appropriate boundary conditions. In the dual field theory language, this amounts to finding the match point in the dimensionless coupling, λ_0 . The point $\lambda = \lambda_0$ can be inferred on the gravity side by seeing when the AdS₃ or BTZ black hole metric looks the same as dS₃, at least in some limit.

One such limit is the near-horizon region of the BTZ black hole at its Hawking-Page phase transition point (where the black hole horizon $r_h = \ell_3$) and the near-horizon region of the dS₃ static patch (where the cosmological horizon is $r_c = \ell_3$) [26]. Using the standard relation between the ADM mass and horizon radius of a (static) BTZ black hole, $8G_3 M_{\text{ADM}} \ell_3^2 = r_h^2$, and the holographic identification $\ell_3 M_{\text{ADM}} = \Delta_n + \bar{\Delta}_n - \frac{c}{12}$, notice at the Hawking-Page phase transition point, where $M_{\text{ADM}} = (8G_3)^{-1}$, the dual CFT satisfies $\Delta_n + \bar{\Delta}_n = \frac{c}{6}$ or $M_n = \frac{c}{12}$ at this transition.

To admit a smooth pure gravity description, the deformed energy spectrum (4.4) is required to be continuous at the matching point $\lambda = \lambda_0$, while maintaining the seed CFT boundary condition, $E_n(\lambda = 0, \eta = 1) = 2\pi M_n/L$. The deformed energy spectrum (for $J_n = 0$) is

$$E_n(\lambda, \eta) = \frac{2\pi}{\lambda L} \left(1 - \sqrt{\eta(1 - 2M_n\lambda)} \right), \quad (4.6)$$

where the integration constant C_1 and ‘-’ are chosen to ensure the seed boundary condition is satisfied. Notice for $\eta = 1$ and $M_n = \frac{c}{12}$, the square root vanishes when $\lambda = \lambda_0 = \frac{6}{c}$. Next, recall the quasi-local Brown-York energy associated with the dS₃ cosmological horizon patch (cf. Eq. (C.12) of [20], where here a shift is owed to the local counterterm appearing in the bulk action (4.5) is included)

$$E_{\text{BY}}^{\text{dS}_3} = \frac{1}{4G_3} \left(\frac{r_B}{\ell_3} + \sqrt{1 - \frac{r_B^2}{\ell_3^2}} \right). \quad (4.7)$$

This energy matches the microscopic spectrum (4.6) for $\eta = -1$, $\lambda = \frac{4G_3\ell_3}{r_B^2}$ when $M_n = \frac{\ell_3}{8G_3} = \frac{c}{12}$; the only difference is that the minus sign in front of the square root in (4.6) should be replaced by a plus sign. Moreover, for $M_n = \frac{c}{12}$ the square root again vanishes when $\lambda_0 = \frac{6}{c}$.

The combined trajectory is then comprised of: (i) pure T $\bar{\text{T}}$ deformation via $\lambda = 0$ to $\lambda = \frac{6}{c}$, choosing the ‘-’ branch, followed by (ii) a T $\bar{\text{T}}$ + Λ_2 deformation from $\lambda = \frac{6}{c}$ to $\lambda \gg 1$,

choosing the ‘+’ branch. The deformed energy spectrum is then piecewise,

$$E_n(\lambda) = \begin{cases} \frac{2\pi}{\lambda L} \left(1 - \sqrt{1 - \frac{\lambda c}{6}} \right) , & \lambda \in [0, \frac{6}{c}] \\ \frac{2\pi}{\lambda L} \left(1 + \sqrt{\frac{\lambda c}{6} - 1} \right) , & \lambda \in [\frac{6}{c}, \infty) \end{cases} \quad (4.8)$$

where the energy is continuous at $\lambda = \frac{c}{6}$. From the bulk perspective the flow is described as follows. First, (i) move the conformal boundary of the BTZ black hole (near its Hawking-Page transition point) inward until $r_B \simeq \ell_3$ ($\lambda = \frac{4G_3}{\ell_3}$). At this point the AdS₃ near horizon geometry is indistinguishable from the near horizon region of dS₃. Then, (ii) move the Dirichlet wall in dS₃ outward toward the pole ($r_B = 0$) filling in the complementary region with the dS₃ static patch including the cosmological horizon.

This patchwise prescription, arguably, allows for a microscopic accounting of the Gibbons-Hawking entropy. Namely, the microstates associated with the $M_n = \frac{c}{12}$ BTZ black hole are attributed to the dS₃ cosmic horizon patch, where the Gibbons-Hawking entropy is given by the Cardy entropy [25, 26]. Indeed,

$$S_{\text{Cardy}} = 2\pi \sqrt{\frac{c}{3} M_n} = \frac{2\pi \ell_3}{4G_3} = S_{\text{GH}} . \quad (4.9)$$

In fact, this argument extends to include the first logarithmic correction $-3 \log(S_{\text{GH}})$ (see [71] for a first principles derivation of the quantum-corrected Gibbons-Hawking entropy). This is due to the fact that the $1/c$ correction to the Cardy entropy is known to reproduce the logarithmic correction to the BTZ black hole entropy [37]. Further, the dS₃ entropy is guaranteed to be finite on account of the deformed spectrum being finite. In [28] the $\overline{\text{T}\overline{\text{T}}} + \Lambda_2$ prescription was generalized to further account for bulk matter fields, going beyond the model-independent pure (semi-classical) gravity sector.

4.2 Generalizing $\overline{\text{T}\overline{\text{T}}} + \Lambda_2$ to arbitrary energies: from BTZ to conical dS₃

Above we briefly reviewed the $\overline{\text{T}\overline{\text{T}}} + \Lambda_2$ flow that is dual to gluing a patch of the BTZ black hole at the Hawking-Page transition point, where $r_h = \ell_3$, to a patch of pure dS₃ geometry. We emphasize that this flow is restricted to a certain energy level, namely where the undeformed CFT starts in a state with energy $M_n = c/12$. On the field theory side, however, the $\overline{\text{T}\overline{\text{T}}} + \Lambda_2$ flow equation allows for a deformed energy spectrum that depends on an *arbitrary* dimensionless energy parameter M_n , given by (4.6) (for $J_n = 0$)

$$E_n(\lambda, \eta, M_n) = \frac{2\pi}{\lambda L} \left(1 \pm \sqrt{\eta(1 - 2M_n\lambda)} \right) . \quad (4.10)$$

This suggests there exists a $\overline{\text{T}\overline{\text{T}}} + \Lambda_2$ flow that starts from an undeformed CFT state with arbitrary energy M_n (instead of setting it equal to $c/12$). In fact, we can combine two different trajectories as before: (i) pure $\overline{\text{T}\overline{\text{T}}}$ deformation from $(\eta = 1, \lambda = 0)$ to $(\eta = 1, \lambda = 1/(2M_n))$ along the ‘-’ branch, followed by (ii) a $\overline{\text{T}\overline{\text{T}}} + \Lambda_2$ deformation from $(\eta = -1, \lambda = 1/(2M_n))$ to large λ along the ‘+’ branch.

Here we describe the holographic dual of this more general flow. We will argue it corresponds to connecting a BTZ black hole with some arbitrary mass $M_{\text{ADM}} (= M_n/\ell_3)$ to a locally dS_3 geometry with a conical defect and the same mass M_{ADM} . The $\text{T}\bar{\text{T}} + \Lambda_2$ flow reviewed in the previous subsection is a special case of this more general flow where $M_{\text{ADM}} = 1/(8G_3)$. A version of this more general $\text{T}\bar{\text{T}} + \Lambda_2$ flow was considered in the original work [26], specifically flows dual to gluing the BTZ geometry to dS_3 with a conical *excess*. Here we consider the case of a conical *defect* — the essential difference being the range of M_{ADM} .

Further, the $\text{T}\bar{\text{T}} + \Lambda_2$ flow for arbitrary M_n is interesting for the purpose of this paper, since, upon a dimensional reduction, it yields a flow that is dual to gluing AdS_2 to dS_2 . We will discuss this in the next subsection, where we also compare this flow to the $\text{T}\bar{\text{T}}$ deformation that is dual to moving from the exterior to the interior in the centaur geometry (considered in section 3). The dimensional reduction of the arbitrary $\text{T}\bar{\text{T}} + \Lambda_2$ flow with arbitrary M_n is more appropriate for comparison with the centaur flow, since in both cases the deformed energy spectrum depends on an arbitrary mass parameter, M_n vs. \mathcal{E}_H , or, equivalently, an arbitrary temperature \tilde{T} . On the other hand, it is difficult to fully compare the $\text{T}\bar{\text{T}} + \Lambda_2$ deformed spectrum with $M_n = c/12$, Eq. (4.8), to the deformed spectrum that is dual to the centaur model, since the former holds only for a specific undeformed CFT energy whereas the latter depends on an arbitrary undeformed energy \mathcal{E}_H . This generalization of $\text{T}\bar{\text{T}} + \Lambda_2$ deformations for arbitrary energies M_n is also interesting in itself (see also [26]).

Let us now describe the three-dimensional bulk dual geometry for the $\text{T}\bar{\text{T}} + \Lambda_2$ flow with arbitrary M_n . Both the static BTZ black hole [59, 60] and the dS_3 geometry with a conical defect, [58, 72] are described by the line element (in Euclidean signature)

$$ds^2 = N(r)d\tau^2 + \frac{dr^2}{N(r)} + r^2d\phi^2, \quad (4.11)$$

where the blackening factor takes the form

$$N(r) = \eta \left(\frac{r^2}{\ell_3^2} - 8G_3M_{\text{ADM}} \right), \quad (4.12)$$

with $\eta = +1$ and $M_{\text{ADM}} > 0$ for the BTZ geometry, and $\eta = -1$ and $0 < M_{\text{ADM}} < 1/(8G_3)$ for conical dS_3 . Conical dS_3 is identical to three-dimensional Schwarzschild-de Sitter (SdS) space, but it does not contain a black hole. Rather, in the global extension of the conical dS_3 geometry there are two conical singularities, one at each pole of a two-sphere. The conical singularities arise due to the presence of point masses at the two poles of dS_3 . For $M_{\text{ADM}} = 1/(8G_3)$ there is no conical defect in dS_3 , and for $M_{\text{ADM}} = 0$ the deficit angle is 2π . For arbitrary M_{ADM} the deficit angle of the conical dS_3 geometry is: $\delta\phi = 2\pi(1 - \sqrt{8G_3M_{\text{ADM}}})$. There is a conical excess in dS_3 for $M_{\text{ADM}} > 1/(8G_3)$, but we discard this solution as unphysical since it corresponds to a negative point mass that is unbounded below.²⁰

²⁰The point mass m is related to the ADM mass via $4G_3m = 1 - \sqrt{8G_3M_{\text{ADM}}}$ [73]. The negative point mass is unbounded for the following reason (see [14, 20]). The cosmological horizon solution is a local maximum

The BTZ geometry has a black hole horizon and the conical dS₃ geometry only has a cosmological horizon. In both cases the horizon radius is given by $r_h = \ell_3 \sqrt{8G_3 M_{\text{ADM}}}$ and hence the horizon entropy equals

$$S_{\text{BH}} = \frac{2\pi r_h}{4G_3} = \frac{2\pi \ell_3}{4G_3} \sqrt{8G_3 M_{\text{ADM}}}. \quad (4.13)$$

Further, for Dirichlet boundaries at fixed r_B the Tolman temperature is

$$\beta_{\text{T}} = \frac{2\pi \ell_3}{\sqrt{8G_3 M_{\text{ADM}}}} \sqrt{\eta \left(\frac{r_B^2}{\ell_3^2} - 8G_3 M_{\text{ADM}} \right)}, \quad (4.14)$$

and the Brown-York quasi-local energy is given by (see also [20, 35])

$$E_{\text{BY}} = \frac{r_B}{4G_3 \ell_3} \left(1 \pm \sqrt{\eta \left(1 - \frac{8G_3 M_{\text{ADM}} \ell_3^2}{r_B^2} \right)} \right). \quad (4.15)$$

The first term in the quasi-local energy arises due to a local counterterm in the gravitational action, which is chosen to be the same for both geometries. The sign in front of the square root is ‘+’ for the quasi-local system $r \in [r_B, \infty)$ in the BTZ geometry and for $r \in [r_B, r_h]$ in conical dS₃, and ‘-’ for the system $r \in [r_h, r_B]$ in BTZ and for $r \in [0, r_B]$ in conical dS₃.

Crucially, the quasi-local energy (4.15) precisely matches with the deformed energy (4.6) due to the holographic dictionary $M_n = M_{\text{ADM}} \ell_3$ and $\lambda = 4G_3 \ell_3 / r_B^2$ (and recall $L = 2\pi r_B$). Thus, the piecewise $\text{T}\bar{\text{T}} + \Lambda_2$ flow for arbitrary M_n described below (4.10) corresponds in the bulk to connecting a patch of the BTZ black hole to a patch of conical dS₃, both with mass M_{ADM} . In particular, the flow consists of two bulk trajectories: (i) moving the conformal boundary of BTZ ($\eta = 1$) until the black hole horizon is reached at $r_B = r_h$ ($\lambda = 1/(2M_{\text{ADM}} \ell_3)$), at which point the near horizon geometry of BTZ is indistinguishable from that of conical dS₃; followed by (ii) moving a Dirichlet boundary inside the static patch of conical dS₃ ($\eta = -1$) toward the pole at $r_B = 0$ ($\lambda = \infty$). We emphasize this piecewise construction is done for each value of M_n . The (dimensionless) deformed energy spectrum along the state-dependent flow thus consists of two pieces and, in terms of the undeformed energy M_n , is given by (recall $\mathcal{E}(\lambda) = E_n(\lambda) r_B$)

$$\mathcal{E}(\lambda, M_n) = \begin{cases} \frac{1}{\lambda} (1 - \sqrt{1 - 2M_n \lambda}) , & \lambda \in [0, \frac{1}{2M_n}] , \\ \frac{1}{\lambda} (1 + \sqrt{2M_n \lambda - 1}) , & \lambda \in [\frac{1}{2M_n}, \infty) . \end{cases} \quad (4.16)$$

rather than a minimum of the Euclidean Einstein gravity action as a function of the mass parameter in the Schwarzschild-de Sitter line element. When the mass parameter is allowed to be negative, the on-shell action is unbounded from below, leading to an arbitrarily large cosmological horizon, and correspondingly, refer to a thermal reservoir whose energy is likewise unbounded from below. We regard such traits as un-physical and therefore discard such solutions. Note, however, negative point mass solutions are in principle valid in the context of gravitational perturbation theory in the presence of timelike Dirichlet walls (see, e.g., the discussion of [74]).

Note that the deformed energy spectrum has each original energy level M_n at $\lambda = 0$ being mapped to different values of λ . In other words, there is not a single theory, at a given λ , which has all of these energy levels as part of its spectrum, unlike standard $\text{T}\bar{\text{T}}$ deformations where the deformed energy spectrum is computed along the flow at a given value of λ . Thus, the resulting spectrum of conical defect states in dS_3 do not live in the same theory.²¹

In terms of the dimensionless (inverse) temperature, the spectrum is

$$\mathcal{E}(\lambda, \tilde{\beta}_{\text{T}}) = \begin{cases} \frac{1}{\lambda} \left(1 - \frac{\tilde{\beta}_{\text{T}}}{\sqrt{\frac{2}{3}\pi^2 c\lambda + \tilde{\beta}_{\text{T}}^2}} \right), & \tilde{\beta}_{\text{T}} \in \left[0, \frac{2\pi}{\sqrt{12M_n/c}} \right], \\ \frac{1}{\lambda} \left(1 + \frac{\tilde{\beta}_{\text{T}}}{\sqrt{\frac{2}{3}\pi^2 c\lambda - \tilde{\beta}_{\text{T}}^2}} \right), & \tilde{\beta}_{\text{T}} \in [0, \infty). \end{cases} \quad (4.17)$$

Note that the transition point in the flow is given by $\tilde{\beta}_{\text{T}} = 0$ or $\lambda = \lambda_0 = 1/(2M_n)$, a state dependent value (reminiscent of Eq. (5.2) [26]). The upper bound on the inverse dimensionless temperature in the upper line arises from the limit $r_B \rightarrow \infty$ (or $\lambda \rightarrow 0$), given by the inverse Hawking temperature divided by ℓ_3 , $\lim_{r_B \rightarrow \infty} \tilde{\beta}_{\text{T}} = \beta_{\text{H}}/\ell_3 = \frac{2\pi}{\sqrt{8G_3 M_{\text{ADM}}}}$, which equals $\frac{2\pi}{\sqrt{12M_n/c}}$ in the boundary theory.

4.3 Dimensional reduction of $\text{T}\bar{\text{T}} + \Lambda_2$

Let us now study a spherical dimensional reduction of the 2D $\text{T}\bar{\text{T}} + \Lambda_2$ flow for arbitrary energies to a flow for a 1D quantum theory. It turns out that the deformed energy spectrum stays the same under this dimensional reduction, just as was the case for the dimensional reduction of the 2D $\text{T}\bar{\text{T}}$ flow to one dimension lower. We show this by dimensionally reducing the 3D bulk action (4.5) to a 2D bulk action of the form (2.1), specifically we find²²

$$I_E = -\frac{1}{16\pi G_N} \int_{\mathcal{M}} d^2x \sqrt{g} (R\Phi + V(\Phi)) - \frac{1}{8\pi G_N} \int_{\partial\mathcal{M}} d\tau \sqrt{h} \Phi (K - \frac{1}{\ell}), \quad (4.18)$$

with a dilaton potential

$$V(\Phi) = \frac{2\eta}{\ell^2} \Phi, \quad (4.19)$$

where we identified $\ell_3 = \ell$. Notice there is no topological term in the 3D to 2D reduction.

The solutions to the dilaton equation of motion for the potential (4.19) take the form (2.6) with

$$N(r) = \eta \frac{r^2 - r_H^2}{\ell^2}, \quad (4.20)$$

the blackening factor corresponding to (i) an AdS_2 black hole ($\eta = +1$), or (ii) the half-reduction of dS_3 space with a conical deficit when $r_H \neq \ell$ ($\eta = -1$). Physically, we are implementing a generalization of the (s-wave reduced) situation studied in [26] where the

²¹We thank Edgar Shaghoulian for emphasizing this point.

²²See Appendix A of [17] for a more general derivation of this type of action.

BTZ black hole has an arbitrary horizon radius, and the (S)dS₃ has a conical deficit. This allows us to carry out a more in-depth thermodynamical analysis for these geometries and the associated dimensional reduction of the T \bar{T} + Λ_2 flow. The geometric interpretation of this flow differs from the interpolating model [22, 66] in that AdS₂ space is glued to a patch of dS₂ space at their respective event horizons instead of the geometries being patched together from the start in a centaur model.

The deformed energy spectrum now follows from inserting the dilaton potential (4.19) into the general formula (2.48)

$$\mathcal{E}(\lambda, \mathcal{E}_0) = \frac{1}{\lambda} \left(1 \pm \sqrt{\eta(1 - 2\lambda\mathcal{E}_0)} \right). \quad (4.21)$$

Here we assume the states in the seed theory can have arbitrary energies \mathcal{E}_0 . Importantly, this expression is equivalent to (4.10) by setting $\mathcal{E}_0 = M_n$. The spectrum with the ‘−’ sign represents the solution of the flow equation that is smoothly connected with the seed theory.

The Tolman temperature corresponding to (4.20) takes the form

$$\beta_T = \frac{\beta_H}{\ell_3} \sqrt{\eta \frac{r_B^2 - r_H^2}{\ell_3^2}}. \quad (4.22)$$

The energy levels (4.21) can be then expressed as

$$\mathcal{E}(\lambda, \tilde{\beta}_T) = \frac{1}{\lambda} \left(1 \pm \frac{\tilde{\beta}_T}{\sqrt{\frac{2}{3}\pi^2 c\lambda + \eta\tilde{\beta}_T^2}} \right), \quad (4.23)$$

where we allow, in principle, the relative \pm sign solutions to the flow equation. However, for the purposes of representing a dimensional reduction of the T \bar{T} + Λ_2 flow, we are interested in analyzing the case with a relative ‘−’ sign in front of the second term for the AdS₂ black hole patch ($\eta = 1$), and a ‘+’ sign for the dS₂ patch ($\eta = -1$), like in (4.16) and (4.17). Figure 10 shows a comparison between the energy expressions (4.16) and (4.17).

The heat capacity (2.46) at fixed λ ,

$$C_\lambda = \mp \frac{1}{\lambda} \frac{\frac{2}{3}\pi^2 c\lambda\tilde{\beta}_T^2}{(\frac{2}{3}\pi^2 c\lambda + \eta\tilde{\beta}_T^2)^{3/2}}, \quad (4.24)$$

is illustrated in Figure 11. As in the centaur model, we find the boundary dual to the AdS₂ black hole that is smoothly connected to the seed theory is thermodynamically stable, while the boundary dual of the cosmic patch dS₂ solution is thermodynamically unstable.

We complete our discussion of the spherical reduction of the T \bar{T} + Λ_2 flow with computing the thermal entropy using the first law $d\mathcal{E} = \tilde{T}dS$ at fixed λ . In the canonical ensemble the entropy is

$$S(\lambda, \tilde{\beta}_T) = S_0 \mp \frac{\frac{2}{3}\pi^2 c\eta}{\sqrt{\frac{2}{3}\pi^2 c\lambda + \eta\tilde{\beta}_T^2}}, \quad (4.25)$$

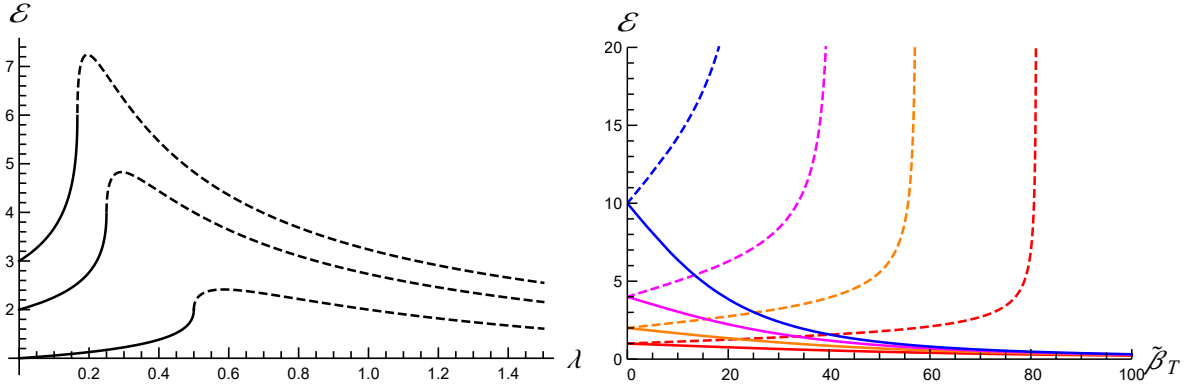


Figure 10: Energy spectrum of the thermal state dual to the s-wave reduction of the $T\bar{T} + \Lambda_2$ flow, **Left:** fixing $\mathcal{E}_0 = 1, 2, 3$ from bottom to top respectively and varying λ (4.21), with a relative $-$ sign for the AdS region, and $+$ for dS), and **Right:** fixing λ and varying $\beta_{\bar{T}}$ (4.23). In both cases, we set $c = 1000$, and in the later case we take (from right to left) $\lambda = 1, .5, .25, .1$; where the solid colored lines indicate $\eta = +1$, and the dashed lines $\eta = -1$.

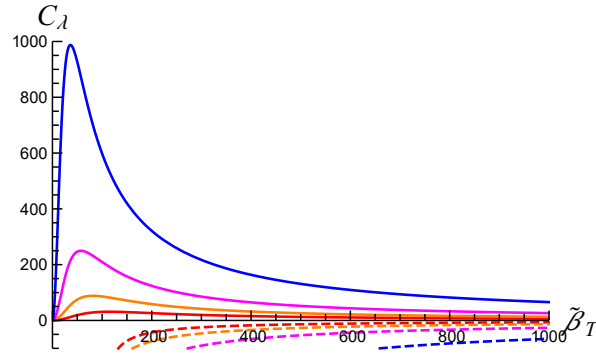


Figure 11: Heat capacity for the thermal state dual to the s-wave reduction of the $T\bar{T} + \Lambda_2$ flow as a function of the dimensionless inverse boundary temperature $\tilde{\beta}_T$. We are using the same parameters as on the right-hand side of Figure 10.

while in the microcanonical ensemble the thermodynamic entropy is given by

$$S(\lambda, \mathcal{E}) = S_0 \mp 2\pi\eta \sqrt{\frac{c}{6} \left(\eta\mathcal{E}(2 - \lambda\mathcal{E}) + \frac{1 - \eta}{\lambda} \right)}. \quad (4.26)$$

Notice there is a lower bound on $\lambda\tilde{T}^2$, given by $1/(\frac{2}{3}\pi^2c)$, along the s-wave reduced $T\bar{T} + \Lambda_2$ flow for $\eta = -1$. These entropy formulae agree with previous expressions derived in subsection 2.4 for the entropies of thermal states dual to an (A)dS₂ patch. That is, by setting $\eta = 1$ and choosing the lower sign in front of the second term in the expressions above we recover Eqs. (2.54) and (2.57), while setting $\eta = 1$ and choosing the upper sign yields Eqs. (2.55) and (2.58). At the interface between the AdS₂ and dS₂ patches, located at the event

horizon of both patches, we have $\lambda = \frac{1}{2\tilde{\epsilon}_0}$, $\tilde{\beta}_T = 0$ and $\mathcal{E} = \frac{1}{\lambda}$, which follows from (4.16) and (4.17). We notice in this case the AdS₂ and dS₂ entropies coincide and the canonical and microcanonical entropies (2.54)-(2.58) reduce to the Cardy formula (2.59).

5 Discussion and Outlook

In this article we revisited the T \bar{T} deformations of theories dual to two-dimensional dilaton theories of gravity [40, 43]. Notably, we carried out a thorough investigation into the microphysical interpretation of the quasi-local thermodynamics of (A)dS₂ JT gravity and the centaur model, which, in our view, had been lacking. In so doing, we uncovered many new formulae for the microscopic theory, including the energy spectrum, heat capacity, and found the entropy of the dual 1D theory obeys a deformed Cardy formula.

We further considered a spherical dimensional reduction of a generalized T \bar{T} + Λ_2 flow connecting a BTZ black hole of arbitrary mass to a locally conical dS₃ spacetime. This led us to a new type of flow connecting (A)dS₂ patches. Geometrically, the flow connects AdS₂ and dS₂ along their respective horizons, in contrast from the centaur model (where dS₂ is glued to a global AdS₂ region). Consequently, the thermal entropy of states dual to the AdS₂ region differs from the thermal entropy of states dual to the AdS₂ region in the centaur model, though both have a Cardy-like form. At the boundary of AdS₂ and at the event horizon the thermal entropy reduces to the standard Cardy formula. Circumstantially, this suggests the deformed boundary theory can be viewed near the boundary *and* the horizon as a dimensional reduction of a 2D CFT, but further work has to be done to examine if this is the case.

The heat capacity of the interpolating system, however, is qualitatively similar to the centaur model. In particular, the boundary dual to the AdS₂ black hole that is smoothly connected to the seed theory is thermodynamically stable, while the boundary dual of the cosmic patch dS₂ solution is unstable. Thus, a signature of the change from AdS to dS is that the heat capacity at a fixed deformation parameter of the Dirichlet wall changes sign.

There are multiple interesting directions to take this work, some of which we list below.

Schwarzian and SYK description. In this article we primarily focused on providing a holographic description of bulk dilaton gravity theories in terms of T \bar{T} -deformed theories. Famously, AdS JT gravity can be understood in terms of a Schwarzian on the AdS₂ boundary, and, at low-energies, is effectively described by a Sachdev-Ye-Kitaev (SYK) model of fermions [75, 76] (see also the review [77]). The partition function of AdS JT gravity with a finite Dirichlet cutoff was evaluated in [78] (see also [79]), and found to precisely match a Schwarzian theory deformed by an operator analogous T \bar{T} -deformations. It would be interesting to directly compute the partition function of the deformed theories considered here, and see if there exists a similar Schwarzian description, expanding on [43]. Moreover, T \bar{T} -like deformations may be directly applied in SYK-type model [80]. Notably, it was found that a pair of uncoupled SYK models with complex coupling constants reproduces the thermody-

namics of the centaur models. It would be interesting to develop an SYK-like description of the (A)dS₂ geometry found from dimensional reduction of $\text{T}\bar{\text{T}} + \Lambda_2$ -deformed theories.

de Sitter JT and DSSYK. The half-reduction model of dS₂ JT gravity arguably has a holographic description in terms of double-scaled SYK (DSSYK) [81–85]. An analysis of 1D $\text{T}\bar{\text{T}}$ deformations in the DSSYK model are addressed in [86, 87]. Notably, the asymptotic boundary conditions and the holographic dictionary relating the deformation parameter and the radial bulk cutoff scale need to be generalized, allowing for complex bulk geometries. Interestingly, phase transitions between thermodynamically stable and unstable configurations can occur depending on the temperature, an aspect not present in our analysis.

Complex eigenvalues and Cauchy slice holography. The appearance of complex eigenvalues in the energy spectrum of T^2 deformations in AdS/CFT (as well as in cosmology [88]) is a crucial component of Cauchy slice holography [88, 89], a proposed duality between bulk gravity and a ‘boundary’ theory that lives on Cauchy slices of the Lorentzian spacetime. Despite the presence of complex energies, bulk unitarity emerges nonetheless, and there exist new types of covariant entropy bounds [90]. Here we explicitly excluded complex energy eigenvalues of the deformed theory. It would be worth adapting this formalism to lower-dimensional models of two-dimensional dilaton gravity, and, as in higher-dimensions reformulate the holographic principle in the language of Wheeler-DeWitt canonical quantization.

Beyond finite Dirichlet walls. In this work we focused on gravity theories with a finite timelike boundary obeying Dirichlet boundary conditions. It is now known, however, such boundary conditions in four-dimensional general relativity do not admit a well-posed initial boundary value problem in Euclidean [91, 92] or Lorentzian signature [93–97].²³ Instead, it has been conjectured that ‘conformal boundary conditions’ (CBCs) — where the trace of the extrinsic curvature and conformal class of the induced metric of the finite boundary are held fixed — supply a well-posed initial boundary value problem [96] (there is in fact a one-parameter family of such boundary conditions [98]). Such CBCs appeared previously in the fluid-gravity paradigm [99, 100], and lead to (conformal) quasi-local thermodynamics [101–103] (see also [104]). In particular, for finite walls obeying CBCs in asymptotically de Sitter backgrounds, the dS static patch is thermally stable (for sufficiently large trace of extrinsic curvature) [102], in stark contrast with the Dirichlet wall case. While the arguments leading to the issues of well-posedness for finite Dirichlet walls do not apply in three-dimensional general relativity or two-dimensional dilaton theories, it would be interesting to develop the analog of $\text{T}\bar{\text{T}}$ -deformations for theories dual to gravity with finite walls obeying CBCs. Such an investigation in the case of three-dimensional gravity was considered in [105]. It would be natural to dimensionally reduce such flows, and develop a holographic description of the conformal quasi-local thermodynamics of the effective two-dimensional dilaton theories [106].

²³Specifically, generic real-valued Dirichlet data do not satisfy the Einstein constraint equations at a finite boundary, nor does the Dirichlet problem have a unique solution (for certain choices of Dirichlet data).

Acknowledgements

We thank Dio Anninos, Eyoab Bahiru, Stefano Baiguera, Damián Galante, Silvia Georgescu, Eleanor Harris, Norihiro Iizuka, Sam van Leuven, Mehrdad Mirbabayi, Andrew Rolph, Sunil Kumar Sake, Edgar Shaghoulian, Vasudev Shyam, Eva Silverstein, Aron Wall, and Nicolò Zenoni for illuminating discussions. We also thank Ricardo Espíndola for initial collaboration on this work. SEAG thanks the University of Amsterdam, the Delta Institute for Theoretical Physics, the International Centre for Theoretical Physics; and the School of Physics of the University of El Salvador for their hospitality and support during several phases of the project, and the Research Foundation - Flanders (FWO) for also providing mobility support (Grant No. K250423N). SEAG and MV also thank the organizers of the XIX Modave summer school, where part of our work was developed. The work of SEAG was partially supported by the FWO Research Project G0H9318N and the inter-university project iBOF/21/084, as well as from the Okinawa Institute of Science and Technology Graduate University. This article was made possible through the support of the ID#62312 grant from the John Templeton Foundation, as part of the ‘The Quantum Information Structure of Spacetime’ Project (QISS), as well as Grant ID# 62423 from the John Templeton Foundation. The opinions expressed in this article are those of the author(s) and do not necessarily reflect the views of the John Templeton Foundation. AS is supported by STFC grant ST/X000753/1. MRV is supported by SNF Postdoc Mobility grant P500PT-206877 and the Spinoza Grant of the Dutch Science Organisation (NWO).

A Flow equations dual to general 2D dilaton gravity

Here, following [40], we provide additional details to the derivation of the flow equation for the effective one-dimensional quantum theory assumed to be dual to a general dilaton theory of gravity. The essential prescription, as presented for holographic CFTs in arbitrary dimensions [62],²⁴ is that the standard $\text{AdS}_{d+1}/\text{CFT}_d$ dictionary relating the bulk gravity and CFT partition functions is taken to hold at finite bulk radial cutoff r_B

$$Z_{\text{EFT}}[r_B; \gamma_{ij}, J] = Z_{\text{grav}}[h_{ij}^B = r_B^2 \gamma_{ij}, \psi_B = r_B^{\Delta-d} J]. \quad (\text{A.1})$$

The left-hand side is the generating function for the (assumed holographic) effective field theory, which need not be a CFT itself, γ_{ij} is the metric describing the field theory geometry, and J is, for simplicity, taken to be a source for a scalar operator \mathcal{O} of dimension Δ . On the right-hand side is the (on-shell) gravitational partition function in an asymptotically AdS background with (Euclidean) metric $ds_{d+1}^2 = g_{\mu\nu} dx^\mu dx^\nu = N(r) dr^2 + r^2 \gamma_{ij} dx^i dx^j$,²⁵ where the bulk metric and bulk scalar field ψ are taken to obey Dirichlet boundary conditions, i.e. fixing the boundary induced metric $h_{ij}(r_B, x) \equiv h_{ij}^B(x)$ and bulk fields $\psi(r_B, x) \equiv \psi_B(x)$. The standard dictionary is recovered in the limit $r_B \rightarrow \infty$. While the status of the proposed

²⁴See also [61, 63, 107] for $\text{T}\bar{\text{T}}$ deformations in arbitrary dimensions.

²⁵Here $N(r) \rightarrow 1/r^2$ near the conformal boundary of AdS.

Dirichlet dictionary (A.1) is questionable for bulk gravity theories in dimensions $d \geq 3$, there appears to be no hurdle for $d = 2$ or, pertinently, $d = 1$.

In a semi-classical limit, the bulk partition function is given by the on-shell Euclidean action, $Z_{\text{grav}} = e^{-I_E}$. The flow of $I_E[r_B]$ is governed by the Hamilton-Jacobi equation with Hamiltonian \mathcal{H} associated with bulk radial evolution.²⁶ Working in this limit and employing the Hamilton-Jacobi equation, the dictionary (A.1) implies the flow equation [62]

$$\partial_{r_B} \hat{I}_{\text{EFT}}(r_B, J) = -\mathcal{H}[r_B^{\Delta-d} J, -r_B^{d-\Delta} \sqrt{\gamma} \mathcal{O}] + \frac{d-\Delta}{r_B} \int dx^d \sqrt{\gamma} J \mathcal{O}, \quad (\text{A.2})$$

for effective (Euclidean) field theory action $\hat{I}_{\text{EFT}} = I_{\text{EFT}} - \int dx^d \sqrt{\gamma} J \mathcal{O}$. Here $\mathcal{O} \equiv \frac{1}{\sqrt{\gamma}} \frac{\delta \hat{I}_{\text{EFT}}}{\delta J}$ at each step along the flow.

Flow equation for 2D dilaton gravity

Bulk flow equation. Following suit, to determine the flow equation for the one-dimensional effective field theory whose energy spectrum is guaranteed to coincide with the quasi-local Brown-York energy of the two-dimensional gravity model in question, one first computes the Hamiltonian constraint of the gravity theory [48, 108] (see also Appendix C of [109])

$$0 = \mathcal{H} = 16\pi G_2 \pi_\Phi \pi^{\tau\tau} - \frac{1}{16\pi G_2} V(\Phi), \quad (\text{A.3})$$

where $\pi^{ab} = -\frac{\sqrt{h}}{16\pi G_2} h^{ab} n^c \nabla_c \Phi$ and $\pi_\Phi = -\frac{\sqrt{h} K}{8\pi G_2}$ are the canonical momenta conjugate to h_{ab} and Φ , respectively, in an ADM split, where $n^c = \sqrt{N} \partial_r^c$ is the unit normal to the timelike boundary. Since it will prove useful momentarily, note that the conjugate momenta π^{ab} features in the (renormalized) quasi-local Brown-York stress-tensor [11] (see, e.g., Appendix C of [50])

$$\tau^{ab} \equiv \frac{2}{\sqrt{h}} \frac{\delta I_E^{\text{on-shell}}}{\delta h_{ab}} = -\frac{1}{8\pi G_2} \left(n^c \nabla_c \Phi - \frac{\Phi}{\ell} \right) h^{ab} = \frac{2}{\sqrt{h}} \left(\pi^{ab} + \frac{\sqrt{h}}{16\pi G_2} \frac{\Phi}{\ell} h^{ab} \right). \quad (\text{A.4})$$

The Brown-York quasi-local energy is

$$E_{\text{BY}} = u_a u_b \tau^{ab} = \tau_\tau^\tau = \frac{\Phi_r r_B}{8\pi G_2 \ell^2} \left(1 - \frac{\ell}{r_B} \sqrt{N(r_B)} \right), \quad (\text{A.5})$$

for unit normal $u^a = N^{-1/2} \partial_r^a$, matching Eq. (2.12).²⁷ The second equality follows from $u_\tau u_\tau \tau^{ab} = h_{\tau\tau} \tau^{\tau\tau} = \tau_\tau^\tau$. Moreover, the momenta π_Φ appears in the scalar operator \mathcal{O}_Φ conjugate to Φ

$$\mathcal{O}_\Phi \equiv \frac{1}{\sqrt{h}} \frac{\delta I_E^{\text{on-shell}}}{\delta \Phi} = -\frac{K}{8\pi G_2} + \frac{1}{8\pi G_2 \ell} = \frac{1}{\sqrt{h}} \left(\pi_\Phi + \frac{\sqrt{h}}{8\pi G_2 \ell} \right). \quad (\text{A.6})$$

²⁶The Hamilton-Jacobi equation describing the bulk radial flow is $\partial_{r_B} I_E[r_B; \psi_B] = -\mathcal{H}[\psi_B, \frac{\delta I_E}{\delta \psi_B}]$.

²⁷To recover the quasi-local energy for the de Sitter JT gravity (2.26), one notes the unit normal $n^c = -\sqrt{N} \partial_r^c$ for the ‘cosmological system’.

This is the bulk analog of the scalar operator associated with source J in the dictionary (A.1). Thus, in terms of these variables, the Hamiltonian constraint (A.3) may be recast as

$$0 = \mathcal{H} = 8\pi G_2 \mathcal{O}_\Phi \tau_\tau^\tau - \frac{\mathcal{O}_\Phi \Phi}{\ell} - \frac{\tau_\tau^\tau}{\ell} + \frac{1}{16\pi G_2} \left[\frac{2\Phi}{\ell^2} - V(\Phi) \right], \quad (\text{A.7})$$

where we used $\sqrt{h} = \sqrt{h_{\tau\tau}}$. Observe the last term vanishes for AdS₂ JT gravity, i.e., $V(\Phi) = 2\Phi/\ell^2$.

The Hamilton-Jacobi equation governing the bulk radial flow is

$$\partial_{r_B} I_E^{\text{on-shell}}[r_B; \Phi_B] = -\mathcal{H} \left[\Phi_B, \frac{\delta I_E^{\text{on-shell}}}{\delta \Phi_B} \right], \quad (\text{A.8})$$

where $\Phi_B \equiv \Phi(r = r_B)$. Let us analyze the left-hand side. A general variation of the dilaton theory (2.1) is

$$\delta I_E = -\frac{1}{2} \int d^2x \sqrt{g} [\mathcal{E}^{\mu\nu} \delta g_{\mu\nu} + \mathcal{E}_\Phi \delta \Phi] + \int d\tau [\pi^{ij} \delta h_{ij} + \pi_\Phi \delta \Phi] + \frac{1}{8\pi G_2} \int d\tau \sqrt{h} \left[\frac{\delta \Phi}{\ell} + \frac{\Phi}{2\ell h} \delta h \right], \quad (\text{A.9})$$

where $\mathcal{E}^{\mu\nu}$ and \mathcal{E}_Φ denote the equations of motion (2.4) and (2.5), respectively. Thus, on-shell,

$$\begin{aligned} \partial_{r_B} I_E[r_B; \Phi_B] &= \int d\tau \sqrt{h} \left[\frac{1}{\sqrt{h}} \left(\pi^{\tau\tau} + \frac{\sqrt{h}\Phi}{16\pi G_2 \ell} h^{\tau\tau} \right) \partial_{r_B} h_{\tau\tau} + \frac{1}{\sqrt{h}} \left(\pi_\Phi + \frac{\sqrt{h}}{8\pi G_2 \ell} \right) \partial_{r_B} \Phi \right] \\ &= \int d\tau \sqrt{h} \left[\frac{1}{2} \tau^{\tau\tau} (\partial_{r_B} h_{\tau\tau}) + \mathcal{O}_\Phi (\partial_{r_B} \Phi) \right]. \end{aligned} \quad (\text{A.10})$$

Boundary flow equation. Now we determine the flow equation for the effective quantum mechanical on the finite boundary by assuming the 2D/1D analog of the dictionary (A.1), together with

$$h_{\tau\tau}^B = (r_B/\ell)^2 \gamma_{\tau\tau}, \quad \tau_{\tau\tau} = r_B \ell^{-1} T_{\tau\tau}, \quad \mathcal{O}_\Phi = r_B^{-2} \ell^2 O, \quad (\text{A.11})$$

where γ_{ij} is the background metric of the 1D quantum mechanical theory, T_{ij} is its stress-energy tensor and O the dual operator of Φ . It follows then

$$\begin{aligned} \partial_{r_B} I_{\text{EFT}} = \partial_{r_B} I_E &= \int d\tau \sqrt{\gamma} \left(\frac{\tau_\tau^\tau}{\ell} + \frac{\mathcal{O}_\Phi \Phi_B}{\ell} \right) \\ &= \int d\tau \sqrt{\gamma} \left(8\pi G_2 \mathcal{O}_\Phi \tau_\tau^\tau + \frac{1}{16\pi G_2} \left[\frac{2\Phi_B}{\ell^2} - V(\Phi_B) \right] \right) \end{aligned} \quad (\text{A.12})$$

where we substituted (A.11) into the bulk relation (A.10) in the first line, and used the Hamiltonian constraint (A.7) to get to the second line. Using the Hamiltonian constraint to replace \mathcal{O}_Φ via

$$\mathcal{O}_\Phi = \frac{\left[\frac{\tau_\tau^\tau}{\ell} - \frac{1}{16\pi G_2} \left(\frac{2\Phi}{\ell^2} - V(\Phi) \right) \right]}{\left(8\pi G_2 \tau_\tau^\tau - \frac{\Phi}{\ell} \right)}, \quad (\text{A.13})$$

gives

$$\partial_{r_B} I_{\text{EFT}} = \int d\tau \sqrt{\gamma} \left[\frac{8\pi G_2 (\tau^\tau)^2 - \frac{\Phi_B}{16\pi G_2 \ell} \left[\frac{2\Phi_B}{\ell^2} - V(\Phi_B) \right]}{\left(8\pi G_2 \tau^\tau - \frac{\Phi_B}{\ell} \right)} \right]. \quad (\text{A.14})$$

Implementing the dictionary (A.11), one finds after a little algebra

$$r_B \partial_{r_B} I_{\text{EFT}} = \int d\tau \sqrt{\gamma} \left[\frac{\lambda^2 (T^\tau_\tau)^2 - \frac{1}{\ell^2} \left(1 - \frac{\ell^2 V(\Phi_B)}{2\Phi_B} \right)}{(\lambda^2 T^\tau_\tau - \lambda \ell^{-1})} \right]. \quad (\text{A.15})$$

Using $r_B \partial_{r_B} = -2\lambda \partial_\lambda$ with $\lambda = 8\pi G_2 \ell^2 / (\Phi_r r_B^2)$, we recover the flow equation (2.47). Note that this flow equation essentially arises from dimensional reduction of a massive gravity action description for a general family of stress-tensor deformations (see Section 3.4 of [61]).

Writing $T^\tau_\tau = E(\lambda)$, the flow equation for the deformed energy spectrum is

$$\partial_\lambda E = \frac{E^2 - (\ell\lambda)^{-2} \left(1 - \frac{\ell^2}{2\Phi_r} \sqrt{\frac{\lambda c}{6}} V\left(\Phi_r \sqrt{\frac{6}{\lambda c}}\right) \right)}{2\ell^{-1} - 2\lambda E}, \quad (\text{A.16})$$

with generic solution

$$E(\lambda) = \frac{1}{\ell\lambda} \left(1 \pm \sqrt{1 + \lambda \ell^2 C_1 + \frac{\lambda}{2} \int_1^\lambda \frac{d\tilde{\lambda}}{\tilde{\lambda}^2} \left[2 - \frac{\ell^2}{\Phi_r} \sqrt{\frac{c\tilde{\lambda}}{6}} V\left(\Phi_r \sqrt{\frac{6}{\tilde{\lambda}c}}\right) \right]} \right). \quad (\text{A.17})$$

for constant C_1 . Introducing a change of integration variable $\tilde{\lambda}$ to y via $y \equiv \Phi_r \sqrt{\frac{6}{c\tilde{\lambda}}}$, such that the integral evaluates to

$$\begin{aligned} \frac{\lambda}{2} \int_1^\lambda \frac{d\tilde{\lambda}}{\tilde{\lambda}^2} \left[2 - \frac{\ell^2}{\Phi_r} \sqrt{\frac{\tilde{\lambda}c}{6}} V\left(\Phi_r \sqrt{\frac{6}{\tilde{\lambda}c}}\right) \right] &= -\frac{\lambda c}{6\Phi_r^2} \int_{\Phi_r \sqrt{\frac{6}{c}}}^y dy [2y - \ell^2 V(y)] \\ &= \lambda - 1 + \lambda \frac{c}{6} \frac{\ell^2}{\Phi_r^2} \int_{\Phi_r \sqrt{\frac{6}{c}}}^y dy V(y). \end{aligned} \quad (\text{A.18})$$

Adjusting constant C_1 , we recover the generic solution (2.49).

References

- [1] G.W. Gibbons and S.W. Hawking, *Cosmological Event Horizons, Thermodynamics, and Particle Creation*, *Phys. Rev. D* **15** (1977) 2738.
- [2] G.W. Gibbons and S.W. Hawking, *Action Integrals and Partition Functions in Quantum Gravity*, *Phys. Rev. D* **15** (1977) 2752.
- [3] T. Banks, *Cosmological breaking of supersymmetry?*, *Int. J. Mod. Phys. A* **16** (2001) 910 [[hep-th/0007146](#)].

- [4] E. Witten, *Quantum gravity in de Sitter space*, in *Strings 2001: International Conference*, 6, 2001 [[hep-th/0106109](#)].
- [5] N. Goheer, M. Kleban and L. Susskind, *The Trouble with de Sitter space*, *JHEP* **07** (2003) 056 [[hep-th/0212209](#)].
- [6] A. Sen, *Extremal black holes and elementary string states*, *Mod. Phys. Lett. A* **10** (1995) 2081 [[hep-th/9504147](#)].
- [7] A. Strominger and C. Vafa, *Microscopic origin of the Bekenstein-Hawking entropy*, *Phys. Lett. B* **379** (1996) 99 [[hep-th/9601029](#)].
- [8] J.W. York, Jr., *Black hole thermodynamics and the Euclidean Einstein action*, *Phys. Rev. D* **33** (1986) 2092.
- [9] B.F. Whiting and J.W. York, Jr., *Action Principle and Partition Function for the Gravitational Field in Black Hole Topologies*, *Phys. Rev. Lett.* **61** (1988) 1336.
- [10] H.W. Braden, J.D. Brown, B.F. Whiting and J.W. York, Jr., *Charged black hole in a grand canonical ensemble*, *Phys. Rev. D* **42** (1990) 3376.
- [11] J.D. Brown and J.W. York, Jr., *Quasilocal energy and conserved charges derived from the gravitational action*, *Phys. Rev. D* **47** (1993) 1407 [[gr-qc/9209012](#)].
- [12] J.D. Brown and J.W. York, Jr., *The Microcanonical functional integral. 1. The Gravitational field*, *Phys. Rev. D* **47** (1993) 1420 [[gr-qc/9209014](#)].
- [13] J.D. Brown, J. Creighton and R.B. Mann, *Temperature, energy and heat capacity of asymptotically anti-de Sitter black holes*, *Phys. Rev. D* **50** (1994) 6394 [[gr-qc/9405007](#)].
- [14] B. Banihashemi and T. Jacobson, *Thermodynamic ensembles with cosmological horizons*, *JHEP* **07** (2022) 042 [[2204.05324](#)].
- [15] S. Carlip and S. Vaidya, *Phase transitions and critical behavior for charged black holes*, *Class. Quant. Grav.* **20** (2003) 3827 [[gr-qc/0306054](#)].
- [16] G. Hayward, *Euclidean action and the thermodynamics of manifolds without boundary*, *Phys. Rev. D* **41** (1990) 3248.
- [17] A. Svesko, E. Verheijden, E.P. Verlinde and M.R. Visser, *Quasi-local energy and microcanonical entropy in two-dimensional nearly de Sitter gravity*, *JHEP* **08** (2022) 075 [[2203.00700](#)].
- [18] P. Draper and S. Farkas, *Euclidean de Sitter black holes and microcanonical equilibrium*, *Phys. Rev. D* **105** (2022) 126021 [[2203.01871](#)].
- [19] D. Anninos and E. Harris, *Interpolating geometries and the stretched dS_2 horizon*, *JHEP* **11** (2022) 166 [[2209.06144](#)].
- [20] B. Banihashemi, T. Jacobson, A. Svesko and M. Visser, *The minus sign in the first law of de Sitter horizons*, *JHEP* **01** (2023) 054 [[2208.11706](#)].
- [21] D. Anninos, S.A. Hartnoll and D.M. Hofman, *Static Patch Solipsism: Conformal Symmetry of the de Sitter Worldline*, *Class. Quant. Grav.* **29** (2012) 075002 [[1109.4942](#)].
- [22] D. Anninos and D.M. Hofman, *Infrared Realization of dS_2 in AdS_2* , *Class. Quant. Grav.* **35** (2018) 085003 [[1703.04622](#)].

- [23] L. Susskind, *De Sitter Holography: Fluctuations, Anomalous Symmetry, and Wormholes*, *Universe* **7** (2021) 464 [[2106.03964](#)].
- [24] S. Leuven, E. Verlinde and M. Visser, *Towards non-AdS Holography via the Long String Phenomenon*, *JHEP* **06** (2018) 097 [[1801.02589](#)].
- [25] V. Shyam, $T\bar{T} + \Lambda_2$ deformed CFT on the stretched dS_3 horizon, *JHEP* **04** (2022) 052 [[2106.10227](#)].
- [26] E. Coleman, E.A. Mazenc, V. Shyam, E. Silverstein, R.M. Soni, G. Torroba et al., *De Sitter microstates from $T\bar{T} + \Lambda_2$ and the Hawking-Page transition*, *JHEP* **07** (2022) 140 [[2110.14670](#)].
- [27] E. Silverstein, *Black hole to cosmic horizon microstates in string/M theory: timelike boundaries and internal averaging*, [2212.00588](#).
- [28] G. Batra, G.B. De Luca, E. Silverstein, G. Torroba and S. Yang, *Bulk-local dS_3 holography: the Matter with $T\bar{T} + \Lambda_2$* , [2403.01040](#).
- [29] A.B. Zamolodchikov, *Expectation value of composite field T anti- T in two-dimensional quantum field theory*, [hep-th/0401146](#).
- [30] F.A. Smirnov and A.B. Zamolodchikov, *On space of integrable quantum field theories*, *Nucl. Phys. B* **915** (2017) 363 [[1608.05499](#)].
- [31] S. Dubovsky, R. Flauger and V. Gorbenko, *Solving the Simplest Theory of Quantum Gravity*, *JHEP* **09** (2012) 133 [[1205.6805](#)].
- [32] A. Cavaglià, S. Negro, I.M. Szécsényi and R. Tateo, *$T\bar{T}$ -deformed 2D Quantum Field Theories*, *JHEP* **10** (2016) 112 [[1608.05534](#)].
- [33] L. McGough, M. Mezei and H. Verlinde, *Moving the CFT into the bulk with $T\bar{T}$* , *JHEP* **04** (2018) 010 [[1611.03470](#)].
- [34] P. Kraus, J. Liu and D. Marolf, *Cutoff AdS_3 versus the $T\bar{T}$ deformation*, *JHEP* **07** (2018) 027 [[1801.02714](#)].
- [35] V. Gorbenko, E. Silverstein and G. Torroba, *dS/dS and $T\bar{T}$* , *JHEP* **03** (2019) 085 [[1811.07965](#)].
- [36] A. Strominger, *Black hole entropy from near horizon microstates*, *JHEP* **02** (1998) 009 [[hep-th/9712251](#)].
- [37] S. Carlip, *Logarithmic corrections to black hole entropy from the Cardy formula*, *Class. Quant. Grav.* **17** (2000) 4175 [[gr-qc/0005017](#)].
- [38] R. Bousso, A. Maloney and A. Strominger, *Conformal vacua and entropy in de Sitter space*, *Phys. Rev. D* **65** (2002) 104039 [[hep-th/0112218](#)].
- [39] J.L. Cardy, *Operator Content of Two-Dimensional Conformally Invariant Theories*, *Nucl. Phys. B* **270** (1986) 186.
- [40] D.J. Gross, J. Kruthoff, A. Rolph and E. Shaghoulian, *$T\bar{T}$ in AdS_2 and Quantum Mechanics*, *Phys. Rev. D* **101** (2020) 026011 [[1907.04873](#)].
- [41] R. Jackiw, *Lower Dimensional Gravity*, *Nucl. Phys. B* **252** (1985) 343.

- [42] C. Teitelboim, *Gravitation and Hamiltonian Structure in Two Space-Time Dimensions*, *Phys. Lett. B* **126** (1983) 41.
- [43] D.J. Gross, J. Kruthoff, A. Rolph and E. Shaghoulian, *Hamiltonian deformations in quantum mechanics, $T\bar{T}$, and the SYK model*, *Phys. Rev. D* **102** (2020) 046019 [[1912.06132](#)].
- [44] J. Maldacena, G.J. Turiaci and Z. Yang, *Two dimensional Nearly de Sitter gravity*, *JHEP* **01** (2021) 139 [[1904.01911](#)].
- [45] M. Cavaglia, *Geometrodynamical formulation of two-dimensional dilaton gravity*, *Phys. Rev. D* **59** (1999) 084011 [[hep-th/9811059](#)].
- [46] J.P.S. Lemos, *Thermodynamics of the two-dimensional black hole in the Teitelboim-Jackiw theory*, *Phys. Rev. D* **54** (1996) 6206 [[gr-qc/9608016](#)].
- [47] J.D.E. Creighton and R.B. Mann, *Quasilocal thermodynamics of two-dimensional black holes*, *Phys. Rev. D* **54** (1996) 7476.
- [48] D. Grumiller and R. McNees, *Thermodynamics of black holes in two (and higher) dimensions*, *JHEP* **04** (2007) 074 [[hep-th/0703230](#)].
- [49] U. Moitra, S.K. Sake, S.P. Trivedi and V. Vishal, *Jackiw-Teitelboim Model Coupled to Conformal Matter in the Semi-Classical Limit*, *JHEP* **04** (2020) 199 [[1908.08523](#)].
- [50] J.F. Pedraza, A. Svesko, W. Sybesma and M.R. Visser, *Semi-classical thermodynamics of quantum extremal surfaces in Jackiw-Teitelboim gravity*, *JHEP* **12** (2021) 134 [[2107.10358](#)].
- [51] E. Witten, *Anti-de Sitter space, thermal phase transition, and confinement in gauge theories*, *Adv. Theor. Math. Phys.* **2** (1998) 505 [[hep-th/9803131](#)].
- [52] I. Savonije and E.P. Verlinde, *CFT and entropy on the brane*, *Phys. Lett. B* **507** (2001) 305 [[hep-th/0102042](#)].
- [53] M.R. Visser, *Holographic thermodynamics requires a chemical potential for color*, *Phys. Rev. D* **105** (2022) 106014 [[2101.04145](#)].
- [54] J. Cotler, K. Jensen and A. Maloney, *Low-dimensional de Sitter quantum gravity*, *JHEP* **06** (2020) 048 [[1905.03780](#)].
- [55] A. Castro, F. Mariani and C. Toldo, *Near-extremal limits of de Sitter black holes*, *JHEP* **07** (2023) 131 [[2212.14356](#)].
- [56] W. Sybesma, *Pure de Sitter space and the island moving back in time*, *Class. Quant. Grav.* **38** (2021) 145012 [[2008.07994](#)].
- [57] J. Kames-King, E.M.H. Verheijden and E.P. Verlinde, *No Page curves for the de Sitter horizon*, *JHEP* **03** (2022) 040 [[2108.09318](#)].
- [58] V. Balasubramanian, J. de Boer and D. Minic, *Mass, entropy and holography in asymptotically de Sitter spaces*, *Phys. Rev. D* **65** (2002) 123508 [[hep-th/0110108](#)].
- [59] M. Banados, C. Teitelboim and J. Zanelli, *The Black hole in three-dimensional space-time*, *Phys. Rev. Lett.* **69** (1992) 1849 [[hep-th/9204099](#)].
- [60] M. Banados, M. Henneaux, C. Teitelboim and J. Zanelli, *Geometry of the (2+1) black hole*, *Phys. Rev. D* **48** (1993) 1506 [[gr-qc/9302012](#)].

- [61] E. Tsoiakidis, *Massive gravity generalization of $T\bar{T}$ deformations*, *JHEP* **09** (2024) 167 [[2405.07967](#)].
- [62] T. Hartman, J. Kruthoff, E. Shaghoulian and A. Tajdini, *Holography at finite cutoff with a T^2 deformation*, *JHEP* **03** (2019) 004 [[1807.11401](#)].
- [63] M. Taylor, *TT deformations in general dimensions*, [1805.10287](#).
- [64] J.D. Brown and J.W. York, Jr., *The Path integral formulation of gravitational thermodynamics*, in *The Black Hole 25 Years After*, pp. 1–24, 1, 1994 [[gr-qc/9405024](#)].
- [65] H.W.J. Bloete, J.L. Cardy and M.P. Nightingale, *Conformal Invariance, the Central Charge, and Universal Finite Size Amplitudes at Criticality*, *Phys. Rev. Lett.* **56** (1986) 742.
- [66] D. Anninos, D.A. Galante and D.M. Hofman, *De Sitter horizons & holographic liquids*, *JHEP* **07** (2019) 038 [[1811.08153](#)].
- [67] D. Anninos and D.A. Galante, *Constructing AdS_2 flow geometries*, *JHEP* **02** (2021) 045 [[2011.01944](#)].
- [68] B. Freivogel, V.E. Hubeny, A. Maloney, R.C. Myers, M. Rangamani and S. Shenker, *Inflation in AdS/CFT* , *JHEP* **03** (2006) 007 [[hep-th/0510046](#)].
- [69] A. Lewkowycz, J. Liu, E. Silverstein and G. Torroba, *$T\bar{T}$ and EE , with implications for $(A)dS$ subregion encodings*, *JHEP* **04** (2020) 152 [[1909.13808](#)].
- [70] E. Silverstein and G. Torroba, *Timelike-bounded dS_4 holography from a solvable sector of the T^2 deformation*, [2409.08709](#).
- [71] D. Anninos, F. Denef, Y.T.A. Law and Z. Sun, *Quantum de Sitter horizon entropy from quasiconformal bulk, edge, sphere and topological string partition functions*, *JHEP* **01** (2022) 088 [[2009.12464](#)].
- [72] S. Deser and R. Jackiw, *Three-dimensional cosmological gravity: Dynamics of constant curvature*, *Annals of Physics* **153** (1984) 405.
- [73] D. Klemm and L. Vanzo, *De Sitter gravity and Liouville theory*, *JHEP* **04** (2002) 030 [[hep-th/0203268](#)].
- [74] T. Andrade, W.R. Kelly, D. Marolf and J.E. Santos, *On the stability of gravity with Dirichlet walls*, *Class. Quant. Grav.* **32** (2015) 235006 [[1504.07580](#)].
- [75] J. Maldacena, D. Stanford and Z. Yang, *Conformal symmetry and its breaking in two dimensional Nearly Anti-de-Sitter space*, *PTEP* **2016** (2016) 12C104 [[1606.01857](#)].
- [76] J. Maldacena and D. Stanford, *Remarks on the Sachdev-Ye-Kitaev model*, *Phys. Rev. D* **94** (2016) 106002 [[1604.07818](#)].
- [77] G. Sárosi, *AdS_2 holography and the SYK model*, *PoS Modave2017* (2018) 001 [[1711.08482](#)].
- [78] L.V. Iliesiu, J. Kruthoff, G.J. Turiaci and H. Verlinde, *JT gravity at finite cutoff*, *SciPost Phys.* **9** (2020) 023 [[2004.07242](#)].
- [79] L. Griguolo, R. Panerai, J. Papalini and D. Seminara, *Nonperturbative effects and resurgence in Jackiw-Teitelboim gravity at finite cutoff*, *Phys. Rev. D* **105** (2022) 046015 [[2106.01375](#)].
- [80] D. Anninos, D.A. Galante and S.U. Sheorey, *Renormalisation Group Flows of the SYK Model*, [2212.04944](#).

- [81] L. Susskind, *Entanglement and Chaos in De Sitter Space Holography: An SYK Example*, *JHAP* **1** (2021) 1 [[2109.14104](#)].
- [82] L. Susskind, *De Sitter Space, Double-Scaled SYK, and the Separation of Scales in the Semiclassical Limit*, [2209.09999](#).
- [83] L. Susskind, *Scrambling in Double-Scaled SYK and De Sitter Space*, [2205.00315](#).
- [84] A.A. Rahman, *dS JT Gravity and Double-Scaled SYK*, [2209.09997](#).
- [85] V. Narovlansky and H. Verlinde, *Double-scaled SYK and de Sitter Holography*, [2310.16994](#).
- [86] S.E. Aguilar-Gutierrez, *T^2 deformations in the double-scaled SYK model: Stretched horizon thermodynamics*, [2410.18303](#).
- [87] S.E. Aguilar-Gutierrez, *Moving boundaries with the double-scaled syk model: t^2 deformations, thermodynamics, and krylov complexity*, To appear.
- [88] G. Araujo-Regado, *Holographic Cosmology on Closed Slices in 2+1 Dimensions*, [2212.03219](#).
- [89] G. Araujo-Regado, R. Khan and A.C. Wall, *Cauchy slice holography: a new AdS/CFT dictionary*, *JHEP* **03** (2023) 026 [[2204.00591](#)].
- [90] R.M. Soni and A.C. Wall, *A New Covariant Entropy Bound from Cauchy Slice Holography*, [2407.16769](#).
- [91] M.T. Anderson, *On boundary value problems for einstein metrics*, *Geometry & Topology* **12** (2008) 2009–2045.
- [92] E. Witten, *A note on boundary conditions in Euclidean gravity*, *Rev. Math. Phys.* **33** (2021) 2140004 [[1805.11559](#)].
- [93] H. Friedrich and G. Nagy, *The Initial boundary value problem for Einstein’s vacuum field equations*, *Commun. Math. Phys.* **201** (1999) 619.
- [94] G. Fournodavlos and J. Smulevici, *The Initial Boundary Value Problem for the Einstein Equations with Totally Geodesic Timelike Boundary*, *Commun. Math. Phys.* **385** (2021) 1615 [[2006.01498](#)].
- [95] G. Fournodavlos and J. Smulevici, *The Initial Boundary Value Problem in General Relativity: The Umbilic Case*, *Int. Math. Res. Not.* **2023** (2023) 3790 [[2104.08851](#)].
- [96] Z. An and M.T. Anderson, *The initial boundary value problem and quasi-local Hamiltonians in General Relativity*, [2103.15673](#).
- [97] D. Anninos, D.A. Galante and B. Mühlmann, *Finite features of quantum de Sitter space*, *Class. Quant. Grav.* **40** (2023) 025009 [[2206.14146](#)].
- [98] X. Liu, J.E. Santos and T. Wiseman, *New Well-Posed boundary conditions for semi-classical Euclidean gravity*, *JHEP* **06** (2024) 044 [[2402.04308](#)].
- [99] I. Bredberg and A. Strominger, *Black Holes as Incompressible Fluids on the Sphere*, *JHEP* **05** (2012) 043 [[1106.3084](#)].
- [100] D. Anninos, T. Anous, I. Bredberg and G.S. Ng, *Incompressible Fluids of the de Sitter Horizon and Beyond*, *JHEP* **05** (2012) 107 [[1110.3792](#)].
- [101] D. Anninos, D.A. Galante and C. Maneerat, *Gravitational observatories*, *JHEP* **12** (2023) 024 [[2310.08648](#)].

- [102] D. Anninos, D.A. Galante and C. Maneerat, *Cosmological observatories*, *Class. Quant. Grav.* **41** (2024) 165009 [[2402.04305](#)].
- [103] D. Anninos, R. Arias, D.A. Galante and C. Maneerat, *Gravitational Observatories in AdS₄*, [2412.16305](#).
- [104] B. Banihashemi, E. Shaghoulian and S. Shashi, *Flat space gravity at finite cutoff*, [2409.07643](#).
- [105] E. Coleman and V. Shyam, *Conformal boundary conditions from cutoff AdS₃*, *JHEP* **09** (2021) 079 [[2010.08504](#)].
- [106] D. Galante, C. Maneerat and A. Svesko., *In preparation*.
- [107] T. Morone, S. Negro and R. Tateo, *Gravity and $T\bar{T}$ flows in higher dimensions*, [2401.16400](#).
- [108] J.L. Davis and R. McNees, *Boundary counterterms and the thermodynamics of 2-D black holes*, *JHEP* **09** (2005) 072 [[hep-th/0411121](#)].
- [109] R. Carrasco, J.F. Pedraza, A. Svesko and Z. Weller-Davies, *Gravitation from optimized computation: Einstein and beyond*, *JHEP* **09** (2023) 167 [[2306.08503](#)].